Fermilab

UPC No. 113

STUDIES ON RADIATION SHIELDING OF ENERGY DOUBLER MAGNETS (II)

H. Edwards, S. Mori and A. Van Ginneken

June 1979

This note continues work reported earlier on calculations of radiation induced quenching problems around the energy doubler. All calculations were performed with 1000 GeV incident protons.

(1) Beam Scraper at Medium Straight Section

Since the momentum dispersion is large at a medium straight section, beam losses associated with RF acceleration failure can be localized there using a beam scraper. Figure 1 shows a beam scraper with an aperture of 4.5 cm(H) by 2 cm(V) and a length of 2m, placed 12m upstream of the Doubler dipole magnets. The beam collimator immediately upstream of the Doubler magnets must have slightly larger effective apertures than the scraper so as not to intercept the primary proton beam. The apertures of the collimator and vacuum chamber plug are chosen to be 5 cm(H) by 3 cm(V) in the present study. (Calculations were made with and without the collimator for comparison.) If horizontal beam dimensions at the scraper and absorber positions are taken into account, the absorber apertures can be narrowed because the proton beam has a larger horizontal amplitude at the scraper. Some results have already been reported.[1] (See Figures S23 and S25 in Supplement 2 of Ref. 1). For runs without the vacuum chamber plug, the vacuum chamber radius was 3.68 to 3.81 cm. Figures 2 and 3 show some of the earlier results. Neither collimator nor vacuum chamber plug were present for the case shown in Figure 2, while both were included for the results given in Figure 3. Figures 4, 5 and 6 show energy density distributions for the vacuum chamber radii extending from 3.18 to 3.31 cm, from 3.18 to 3.44 cm, and from 3.18 to 3.57 cm. The beam strikes inside ($\phi = 0$) and outside ($\phi = \pi$) edges of the scraper with an incident angle of 0 mrad.

Energy density distributions in the magnet coils depend strongly on details of the shielding at the magnets. When the collimator upstream of the magnets is not present in the calculation, a sharp peak appears at the upstream end of the magnets. With the vacuum chamber plug absent the second peak appears about 6m (9m) for $\phi = \pi(0)$ from the upstream end of the magnet and is due to high energy photons from neutral pion decay. With the plug present, the peak corresponding to neutral pion production disappears and the energy density has a rather broad peak about 3m into the magnet. Table I summarizes peak energy densities in the coil for a shallow radial range (3.81 cm to 4.40 cm) for various configurations. It can be seen that the plug reduces the maximum energy density further to about 0.006 GeV/(cm^3 · interacting proton). This means that about 10^{11} interacting protons would cause a maximum energy density at the magnet coils of 12 mj/g. Also given are peak energy densities for an arrangement proposed by T.Collins[2] in which the upstream dipoles are replaced by two 3-m long dipoles with a 4 inch rperture and equipped with absorbers. The maximum energy density for this case is very similar to that with the plug.

If magnets with larger apertures are substituted for the two upstream magnets (6m each), the maximum energy density can be reduced considerably. Figure 7 shows the maximum energy density as a function of coil radius at $\phi = 0$ and π with the vacuum chamber plug present. The maximum energy density with 4 inch aperture magnet coils is about 0.0025 GeV/(cm^3 · interacting proton). Similarly, the maximum energy should be smaller for a vacuum chamber plug with a smaller aperture.

In conclusion the maximum energy density at the Doubler magnet coils downstream of the beam scraper at the medium straight section can be reduced to about 0.006 GeV/(cm^3 · interacting proton) using a 5 cm(H) x 3 cm(V) vacuum chamber plug. If, in addition, magnets with a larger aperture are substituted for the two regular magnets following the medium straight section then the maximum energy density can be as low as 0.002 GeV/(cm^3 · interacting proton) or less.

(2) Electrostatic Septum Wires

Some calculations about radiation problems due to scattering off the electrostatic septum wires have already been reported.[1] A beam dump consisting of four conventional magnets is introduced to take the brunt of the energy deposited by the scattered particles. Figure 8 shows the arrangement of the earlier study. The horizontal bump results were calculated both for inward

and outward beam deflection. It was concluded that (a) a vertical bump is likely more efficient than a horizontal bump since vertical apertures can be made much smaller (b) the septum is preferably placed downstream of the first bump magnet to achieve a larger spread in the angles and positions of (positive) off-momentum particles at the front of the doubler string.

We report here results for a more realistic geometry including superconducting quadrupole magnets as shown in Figure 9. Energy density distributions in both quadrupole and dipole strings were calculated for two sets of collimator and plug aperatures given in Table II. Figures 10 and 11 show energy density distributions for the narrow aperture configurations and Figures 12 and 13 for the wide aperture configuration. Although the narrow aperture configuration gives better radiation shielding, the wide aperture configuration seems to be more practical from the standpoints of construction and alignment. For the wide aperture configuration the maximum energy density in the Doubler magnet coils is 5×10^{-5} GeV/(cm^3 · incident proton on septum wires). For an energy deposition limit of 1 mj/g, about 10^{12} protons are allowed to strike the septum wires. Therefore, the maximum number of protons can be extracted is about 4×10^{13} protons/pulse when the extraction efficiency is 97.5%, i.e., 2.5% of protons strike septum wires. If necessary, the energy deposition in the Doubler magnet coils can be further recuded by using beam collimators with smaller apertures or by using a few large aperture magnets downstream of the beam bump magnets.

(3) Lambertson Septum Magnets

Previous studies[1] about radiation problems due to scattering from the Lambertson septum magnets were also made for a simple geometry which omitted all quadrupole magnets. Energy density distributions in downstream Doubler magnets were found to depend strongly on beam conditions. When the proton beam strikes the upstream surface of the septum perpendicularly, the energy density in the downstream Doubler magnet coils is relatively small because the Lambertson magnets have enough absorbing material at the septum region in the forward direction. On the other hand, when the proton beam strikes the side surface of the septum with a small incident angle ($\sim$30 μad), the energy density in the downstream magnet coils becomes substantial.

Figures 14 through 18 show results for a more realistic geometry which includes superconducting quadrupole magnets. The protons were assumed to strike the side surface of the septum from the direction of the

field free region. They were distributed uniformly along the first 3.2m of the septum with an angle of incidence of 30 μrad. Figure 19 shows one of the earlier results for the simple geometry under the same beam conditions. There was no collimator assumed present.

Figures 14 and 17 show energy density distributions in the quadrupole string with and without an iron collimator, 5 cm(H) by 3 cm (V) and 2m in length, respectively, upstream of the quadrupole string. The maximum energy densities without collimator are similar to the upstream peaks seen in earlier calculations, as shown in Figure 19. The peak values in the first quadrupole were suppressed by an order of magnitude due to the collimator, but the peaks in the second quadrupole were affected much less. An additional collimator may be needed between the two quadrupole magnets. Energy density distributions in the dipole string are shown in Figures 15 and 16 for vacuum chamber radii from 3.68 to 3.81 cm and from 3.18 to 3.31 cm, respectively. No collimator was assumed to be present upstream of the quadrupole string. Distributions with a collimator present are shown in Figure 18 for a vacuum chamber radius from 3.68 to 3.81 cm. They are similar to the distributions around the second maxima for the geometry without quadrupoles (Figure 19).

In summary those preliminary results indicate that the Lambertson magnet areas for both normal extraction and beam abort may not require anything more than simple beam collimators and vacuum chamber plugs for the downstream Doubler magnets. Detailed studies which include angle and position distributions at the Lambertson magnets for protons scattered from the electrostatic septum wires are in progress.

(4) Mini-Straight Section

We previously discussed the case where the proton beam strikes the upstream end of the Doubler dipole magnet[1]. We report here on a similar problem when the proton beam strikes a quadrupole magnet at a mini-straight section. Figure 20 shows a typical configuration. Figures 21 through 30 show the energy density in quadrupole and dipole magnet coils as a function of azimuthal angle and coil radius. For some cases an iron collimator with the horizontal aperture of 6.2 cm is placed immediately upstream of the downstream Doubler dipole. Other conditions are indicated in the legend of figures. The vacuum chamber radius of the quadrupole magnet is from 3.68 to 3.81 cm. Table III summarizes the maximum energy deposition in the correction coils and main coils of the quadrupole magnet as well as in the two radial ranges of the dipole magnet coils. The maximum energy deposition in both the sets of coils of the

quadrupole magnet increases as the scraper length increases from 2 to 20 cm, it decreases substantially for a scraper length of 100 cm. Therefore, the collimator upstream of the dipole must be substantially long ($\gtrsim$ 30 cm) to be effective for shielding. A thin collimator ($\lesssim$ 10 cm) can increase the maximum energy density in the downstream Doubler magnet. We also studied the case in which the scraper was placed inside the vacuum chamber of the quadrupole magnet. The energy deposition in the quadrupole magnet coils is quite large.

References

1. H.Edwards, S.Mori and A.Van Ginneken, Studies on Radiation Shielding of Energy Doubler Magnets (1), Fermi National Accelerator Laboratory UPC No. 30, December 27, 1978.

   H.Edwards, S.Mori and A.Van Ginneken, Supplement to UPC 30, Fermi National Accelerator Laboratory UPC No. 40, January 12, 1979.

   H.Edwards, S.Mori and A.Van Ginneken, Supplement 2, of UPC No. 40, February 1979.

2. T.Collins, "Charged Particle Distributions Estimate", Internal Report 1978.

Maximum Energy Deposition in Doubler Magnets Due to Scattering from a Beam Scraper at a Medium Straight Section in Unit of GeV / (cm^3 x Interacting Proton) for the Beam Energy of 1000 GeV.

Vacuum Chamber Radius (cm)	Collimator	ϕ	Angular Range (Radians) 0.000 - 0.100		3.042 - 3.142	
			Upstream Peak	2nd Peak	Upstream Peak	2nd Peak
3.68 - 3.81	no	0				
	no	π	.019	.008	-	.041
3.18 - 3.31	yes	0	-	.012	-	.030
	yes	π	-	.006	-	.024
3.18 - 3.44	yes	0	-	.010	-	.023
	yes	π	-	.005	-	.018
3.18 - 3.57	yes	0	-	.009	-	.017
	yes	π	-	.005	-	.012
Plug	no	0	-	.005	.019	.007
	no	π	.015	.005	-	.005
	yes	0	-	.006	-	.006
	yes	π	-	.005	-	.006
T. Collins' Scheme	-	0	-	.007	-	.007
	-	π	-	.008	-	.007

TABLE I.

TABLE II. Collimator Dimensions (Full Width In cm) For Beam Bump Magnets And Doubler Quadrupole And Dipole Magnets At Extraction Electrostatic Septum.

Aperture	Direction	B2 and B3	B4	Quad Plug	Dipole Plug
I. Narrow	Horizontal	5.0	3.4	4.0	5.0
	Vertical	1.1	2.0	3.0	2.0
II. Wide	Horizontal	5.0	3.4	4.0	5.0
	Vertical	2.2	4.0	6.0	4.0

TABLE III. Maximum Energy Deposition In The Unit Of GeV/(cm^3.Interacting Proton) At The Mini-Straight Section.

Figure	Scraper Length (cm)	Dipole Inner Vacuum Chamber Radius (cm)	ϕ (rad)	θ_{Beam} (mrad)	Collimator Length Upstream Of Dipole (cm)	Coil Radial Ranges (cm)			
						Quadrupole Magnet		Dipole Magnet	
						3.81-4.07 (Correction Coils)	4.49-5.00 (Main Coils)	3.81-4.40	4.40-5.00
21	2	3.68	0	0.7	-	0.26	0.05	0.10	0.02
22	2	3.68	π	-0.7	-	0.17	0.05	0.11	0.03
23	10	3.68	0	0.7	-	0.33	0.12	0.05	0.03
24	10	3.68	0	0.7	10	0.33	0.12	0.07	0.05
25	10	3.18	0	0.7	30	0.33	0.12	0.04	0.04
26	10	3.68	π	-0.7	-	0.33	0.10	0.06	0.03
27	20	3.68	0	0.7	-	0.35	0.14	0.04	0.03
28	20	3.68	π	-0.7	-	0.33	0.15	0.05	0.03
29	100	3.68	0	0.7	-	0.10	0.04	0.013	0.012
30	100	3.68	π	-0.7	-	0.04	0.03	0.016	0.013

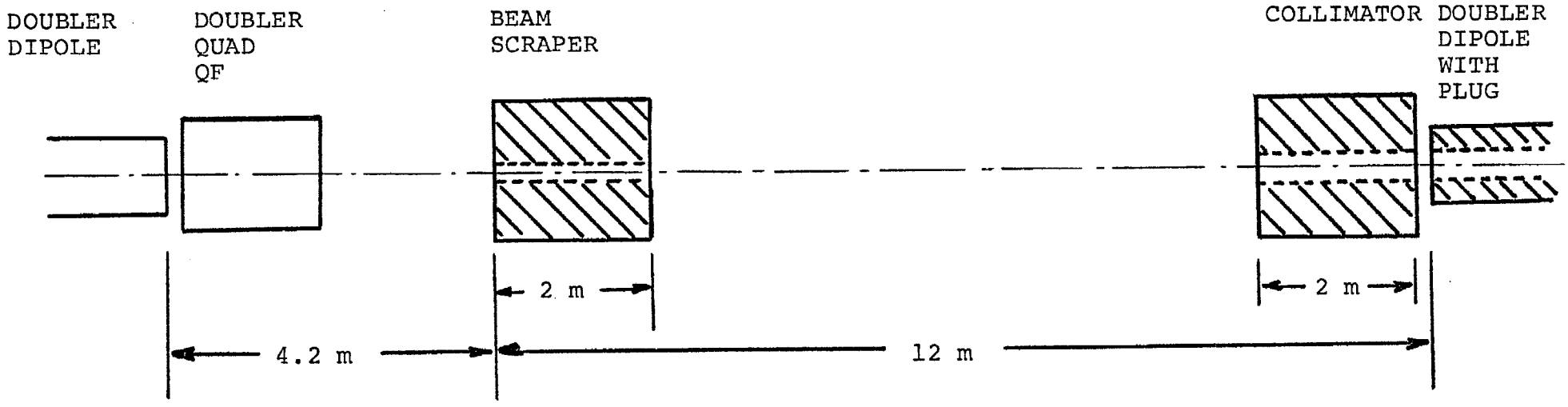

BEAM SCRAPER ARRANGEMENT AT MEDIUM STRAIGHT SECTION

BEAM SCRAPER APERTURE: 4.5 cm(H) by 2 cm(V)
COLLIMATOR APERTURE: 5 cm(H) by 3 cm(V)
PLUG APERTURE: 5 cm(H) by 3 cm(V)

Figure 1.

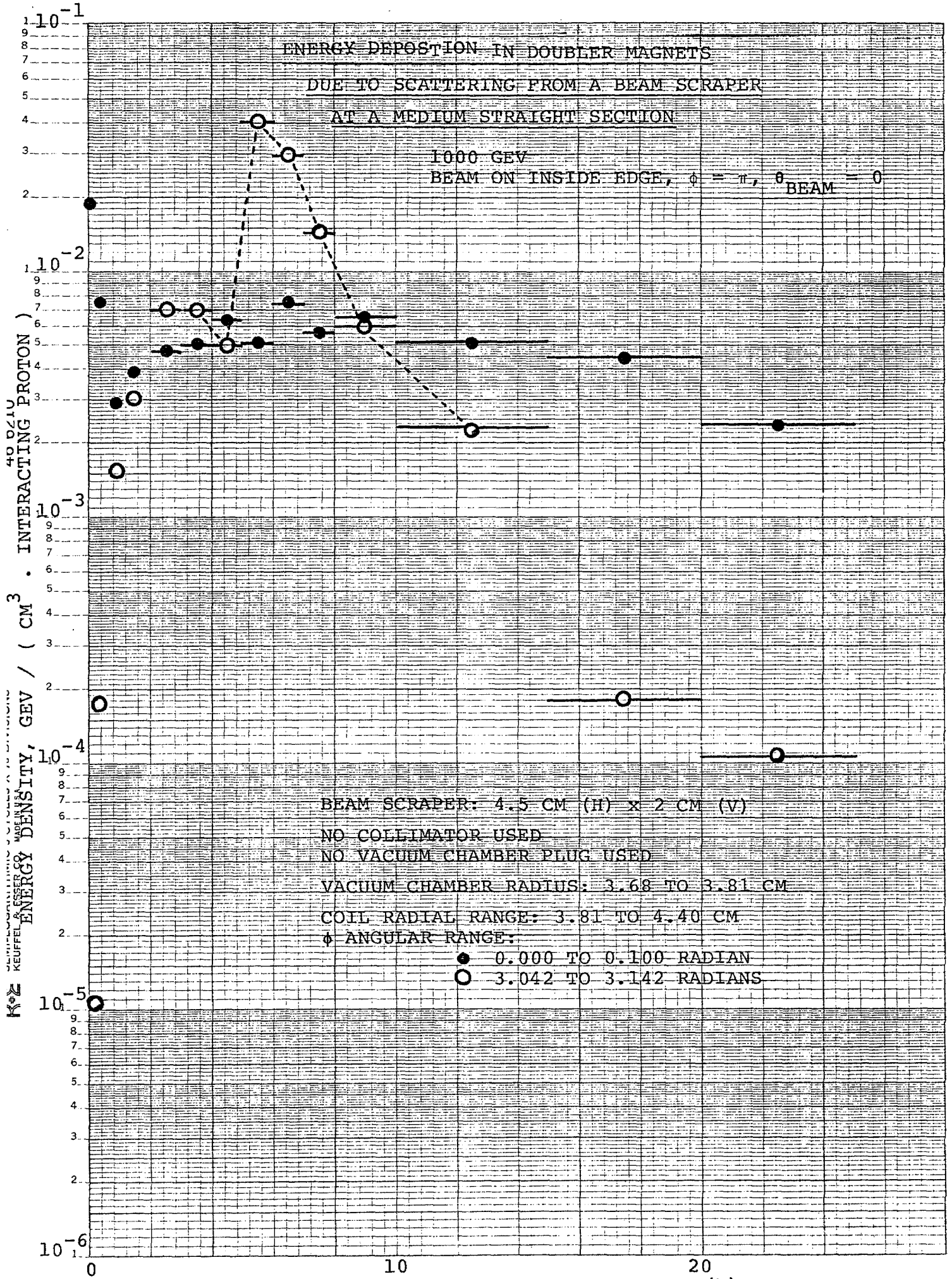
ENERGY DEPOSTION IN DOUBLER MAGNETS
DUE TO SCATTERING FROM A BEAM SCRAPER
AT A MEDIUM STRAIGHT SECTION
1000 GEV
BEAM ON INSIDE EDGE, $\phi = \pi$, $\theta_{BEAM} = 0$
BEAM SCRAPER: 4.5 CM (H) x 2 CM (V)
NO COLLIMATOR USED
NO VACUUM CHAMBER PLUG USED
VACUUM CHAMBER RADIUS: 3.68 TO 3.81 CM
COIL RADIAL RANGE: 3.81 TO 4.40 CM
ϕ ANGULAR RANGE:
0.000 TO 0.100 RADIAN
3.042 TO 3.142 RADIANS
ENERGY DENSITY, GEV / (CM^3 . INTERACTING PROTON)
DISTANCE FROM UPSTREAM END OF MAGNET (M)
0
10
20
10^{-1}
10^{-2}
10^{-3}
10^{-4}
10^{-5}
10^{-6}

Figure 2.

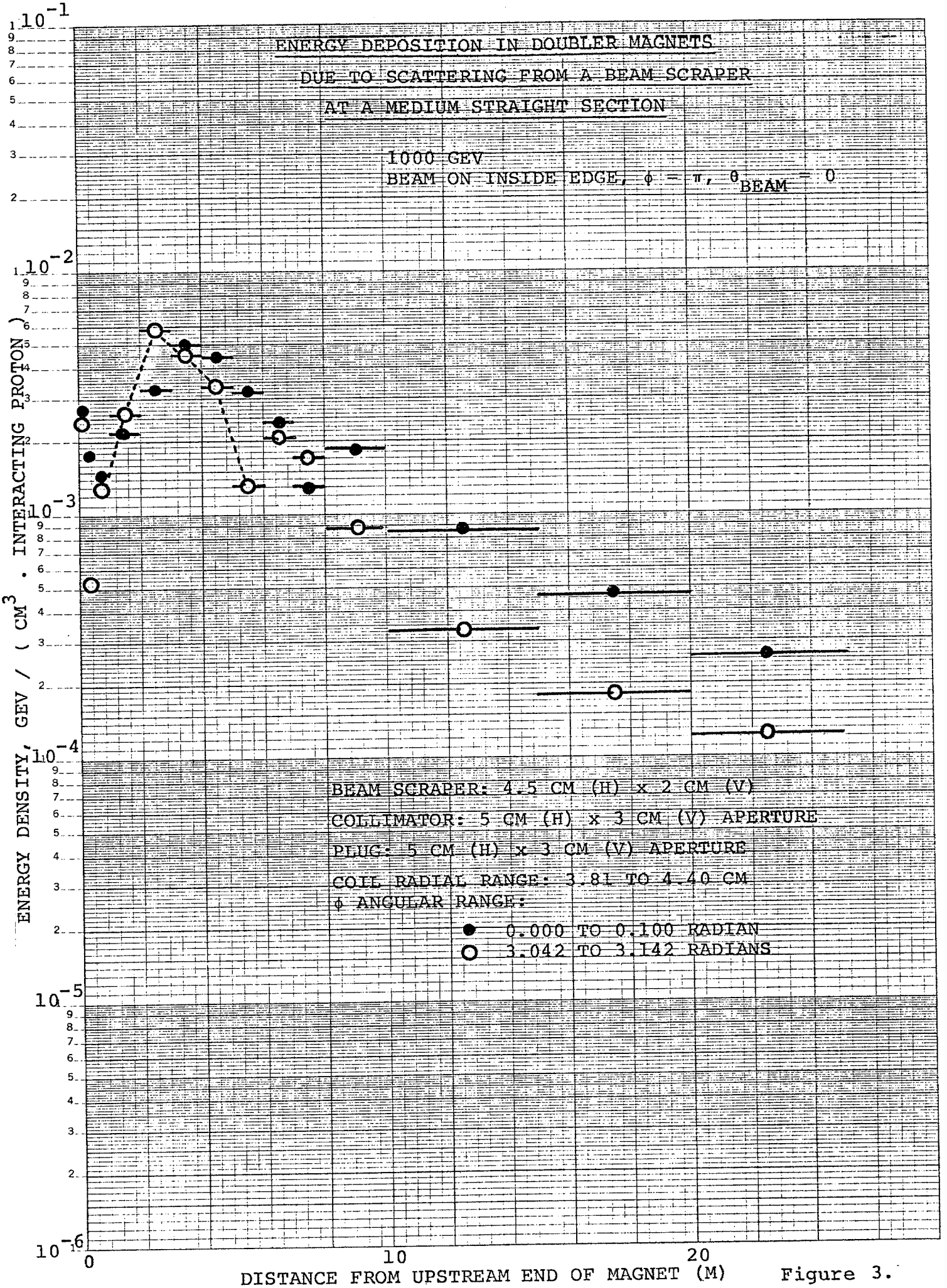
ENERGY DEPOSITION IN DOUBLER MAGNETS
DUE TO SCATTERING FROM A BEAM SCRAPER
AT A MEDIUM STRAIGHT SECTION
1000 GEV
BEAM ON INSIDE EDGE, $\phi = \pi$, $\theta_{BEAM} = 0$
ENERGY DENSITY, GEV / (CM^3 · INTERACTING PROTON)
10^{-1}
10^{-2}
10^{-3}
10^{-4}
10^{-5}
10^{-6}
BEAM SCRAPER: 4.5 CM (H) x 2 CM (V)
COLLIMATOR: 5 CM (H) x 3 CM (V) APERTURE
PLUG: 5 CM (H) x 3 CM (V) APERTURE
COIL RADIAL RANGE: 3.81 TO 4.40 CM
ϕ ANGULAR RANGE:
● 0.000 TO 0.100 RADIAN
○ 3.042 TO 3.142 RADIANS
0
10
20
DISTANCE FROM UPSTREAM END OF MAGNET (M)

Figure 3.

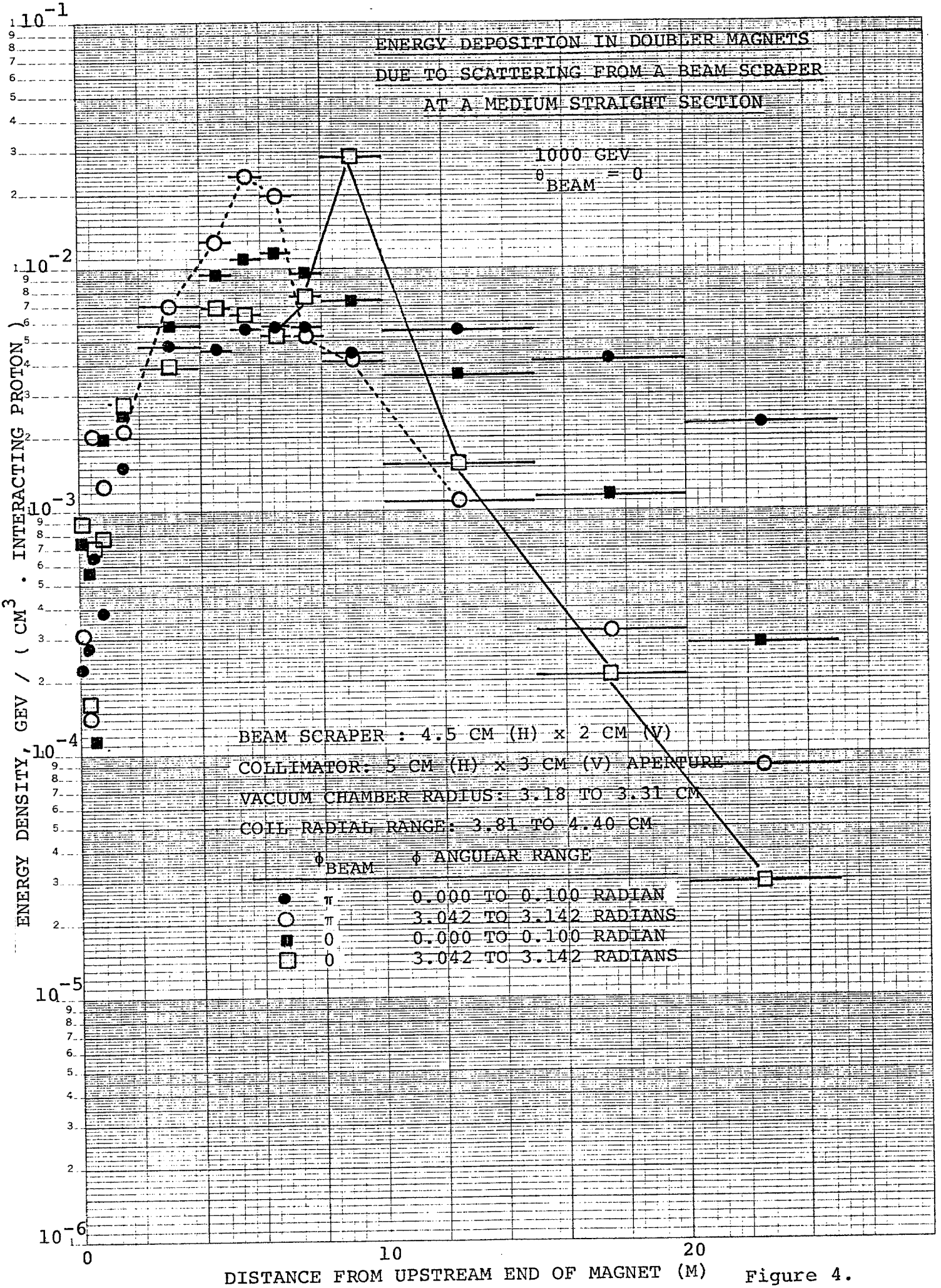
ENERGY DEPOSITION IN DOUBLER MAGNETS
DUE TO SCATTERING FROM A BEAM SCRAPER
AT A MEDIUM STRAIGHT SECTION
1000 GEV
$\theta_{BEAM} = 0$
BEAM SCRAPER : 4.5 CM (H) x 2 CM (V)
COLLIMATOR: 5 CM (H) x 3 CM (V) APERTURE
VACUUM CHAMBER RADIUS: 3.18 TO 3.31 CM
COIL RADIAL RANGE: 3.81 TO 4.40 CM
ϕ_{BEAM} ϕ ANGULAR RANGE
● π 0.000 TO 0.100 RADIAN
○ π 3.042 TO 3.142 RADIANS
■ 0 0.000 TO 0.100 RADIAN
□ 0 3.042 TO 3.142 RADIANS
ENERGY DENSITY, GEV / (CM^3 · INTERACTING PROTON)
10^{-1}
10^{-2}
10^{-3}
10^{-4}
10^{-5}
10^{-6}
0
10
20
DISTANCE FROM UPSTREAM END OF MAGNET (M)

Figure 4.

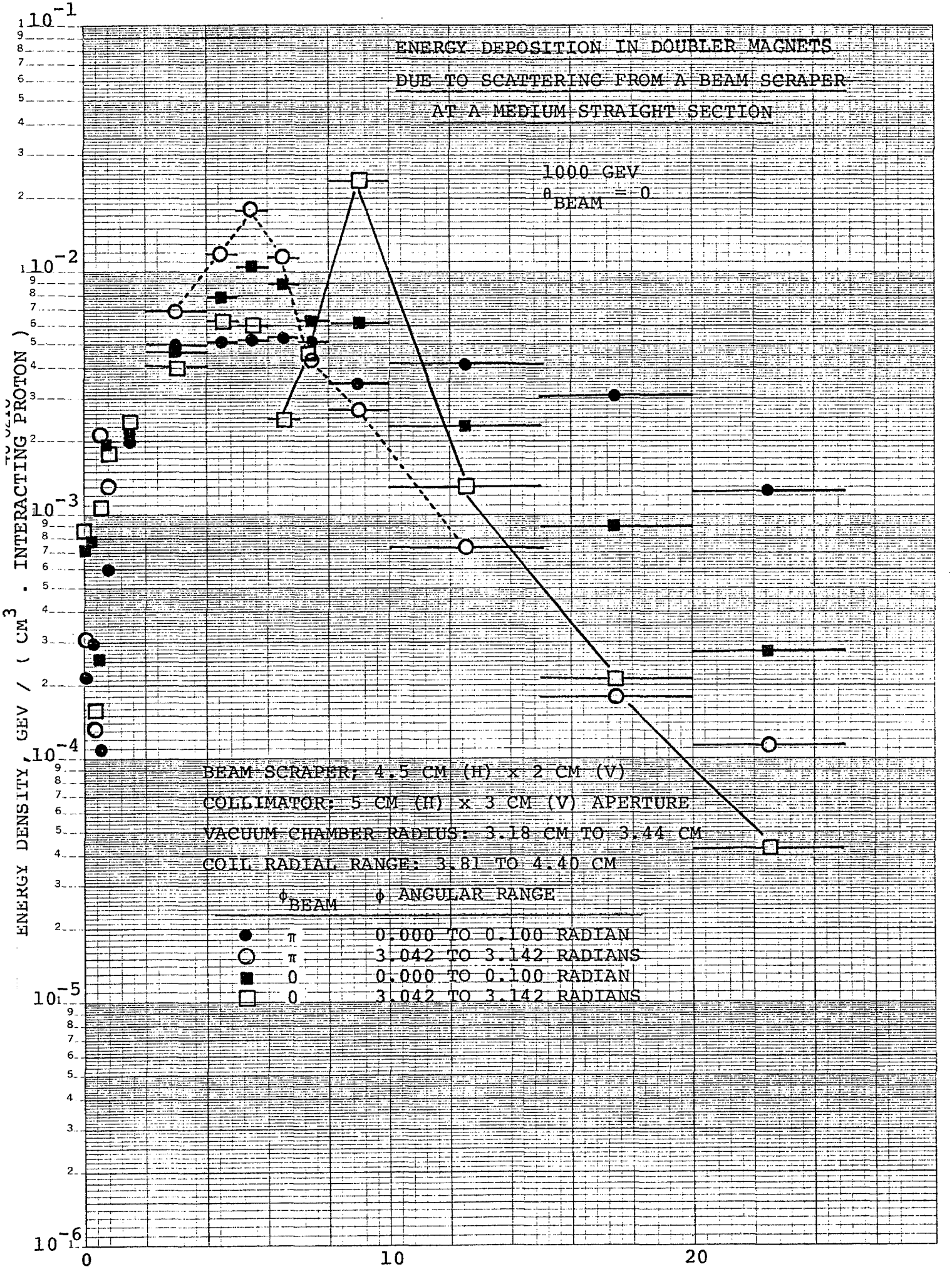
ENERGY DEPOSITION IN DOUBLER MAGNETS
DUE TO SCATTERING FROM A BEAM SCRAPER
AT A MEDIUM STRAIGHT SECTION
1000 GEV
$\theta_{BEAM} = 0$
BEAM SCRAPER: 4.5 CM (H) x 2 CM (V)
COLLIMATOR: 5 CM (H) x 3 CM (V) APERTURE
VACUUM CHAMBER RADIUS: 3.18 CM TO 3.44 CM
COIL RADIAL RANGE: 3.81 TO 4.40 CM
ϕ_{BEAM} φ ANGULAR RANGE
● π 0.000 TO 0.100 RADIAN
○ π 3.042 TO 3.142 RADIANS
■ 0 0.000 TO 0.100 RADIAN
□ 0 3.042 TO 3.142 RADIANS
ENERGY DENSITY, GEV / (CM^3 . INTERACTING PROTON)
10^{-1}
10^{-2}
10^{-3}
10^{-4}
10^{-5}
10^{-6}
0
10
20
DISTANCE FROM UPSTREAM END OF MAGNET (M)

Figure 5.

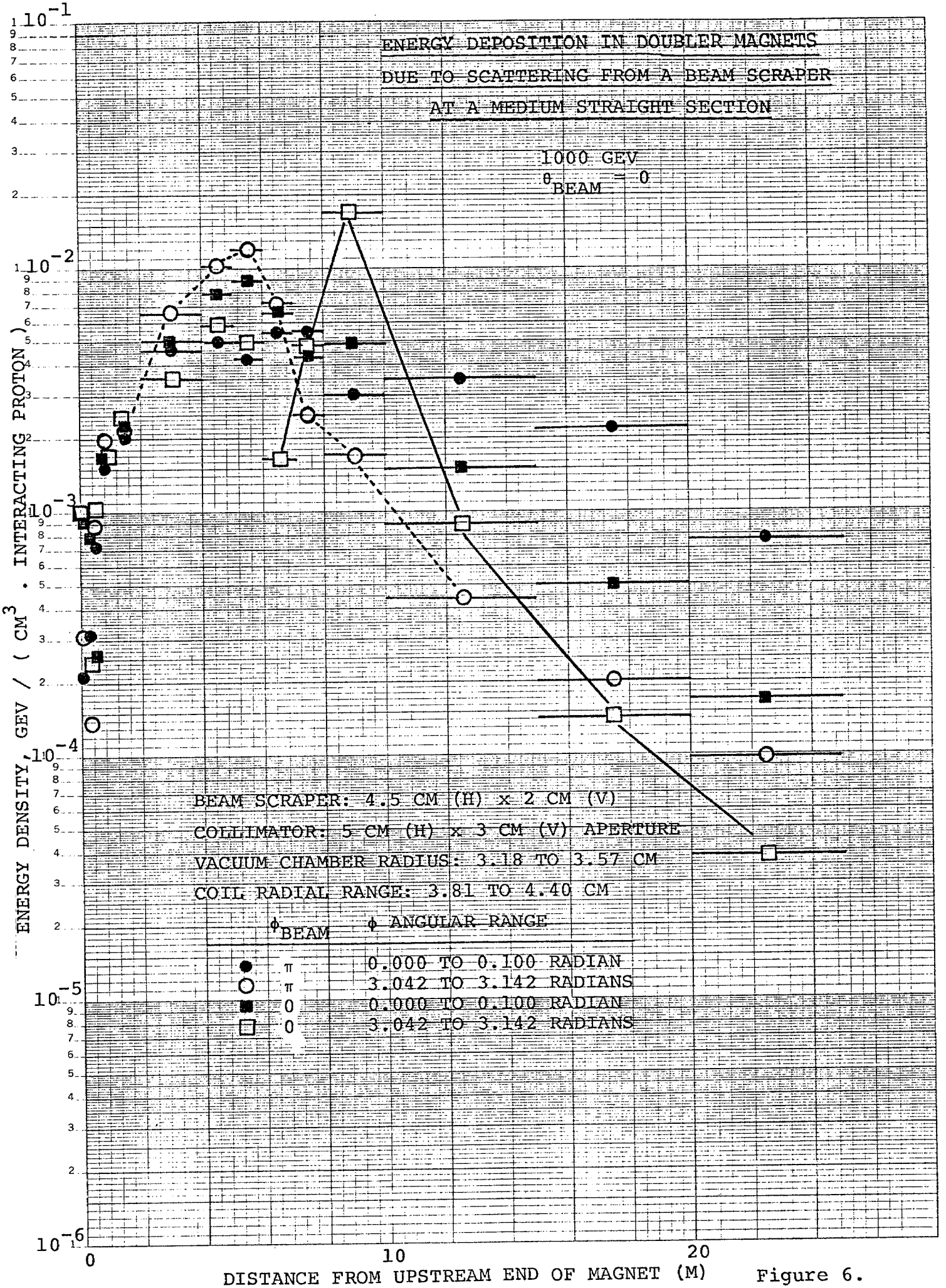
ENERGY DEPOSITION IN DOUBLER MAGNETS
DUE TO SCATTERING FROM A BEAM SCRAPER
AT A MEDIUM STRAIGHT SECTION
1000 GEV
$\theta_{BEAM} = 0$
ENERGY DENSITY, GEV / (CM^3 • INTERACTING PROTON)
10^{-1}
10^{-2}
10^{-3}
10^{-4}
10^{-5}
10^{-6}
BEAM SCRAPER: 4.5 CM (H) x 2 CM (V)
COLLIMATOR: 5 CM (H) x 3 CM (V) APERTURE
VACUUM CHAMBER RADIUS: 3.18 TO 3.57 CM
COIL RADIAL RANGE: 3.81 TO 4.40 CM
ϕ_{BEAM} ϕ ANGULAR RANGE
● π 0.000 TO 0.100 RADIAN
○ π 3.042 TO 3.142 RADIANS
■ 0 0.000 TO 0.100 RADIAN
□ 0 3.042 TO 3.142 RADIANS
0
10
20
DISTANCE FROM UPSTREAM END OF MAGNET (M)

Figure 6.

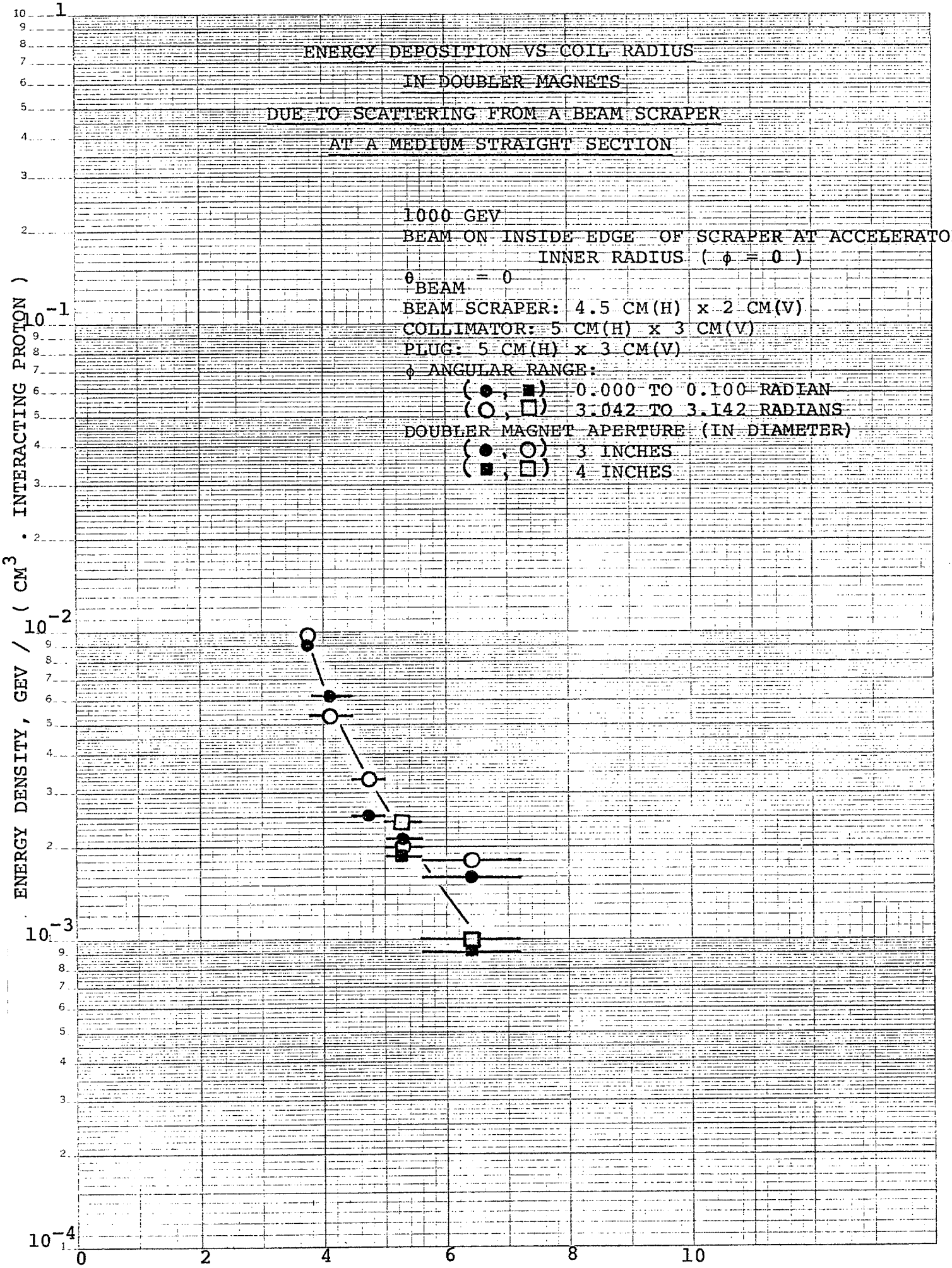
ENERGY DEPOSITION VS COIL RADIUS
IN DOUBLER MAGNETS
DUE TO SCATTERING FROM A BEAM SCRAPER
AT A MEDIUM STRAIGHT SECTION
1000 GEV
BEAM ON INSIDE EDGE OF SCRAPER AT ACCELERATOR
INNER RADIUS (φ = 0)
θ BEAM = 0
BEAM SCRAPER: 4.5 CM(H) x 2 CM(V)
COLLIMATOR: 5 CM(H) x 3 CM(V)
PLUG: 5 CM(H) x 3 CM(V)
φ ANGULAR RANGE:
(●, ■) 0.000 TO 0.100 RADIAN
(○, □) 3.042 TO 3.142 RADIANS
DOUBLER MAGNET APERTURE (IN DIAMETER)
(●, ○) 3 INCHES
(■, □) 4 INCHES
ENERGY DENSITY, GEV / (CM3 • INTERACTING PROTON)
MAGNET COIL RADIUS (CM)
0
2
4
6
8
10
1
10-1
10-2
10-3
10-4

Figure 7.

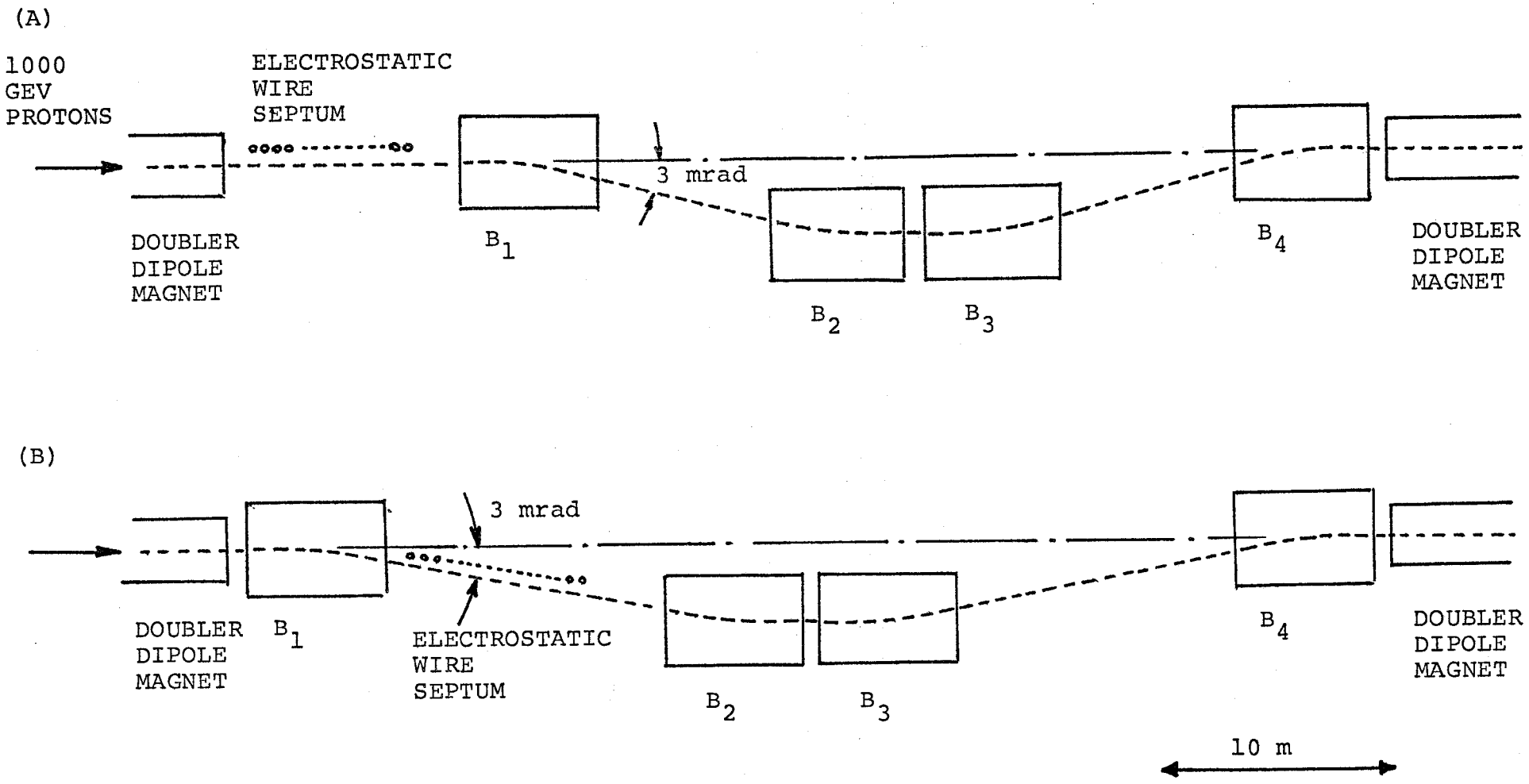

EXTRACTION ELECTROSTATIC WIRE SEPTUM
AND FOUR MAGNET BUMP ARRANGEMENT
(HORIZONTAL OR VERTICAL)

Figure 8.

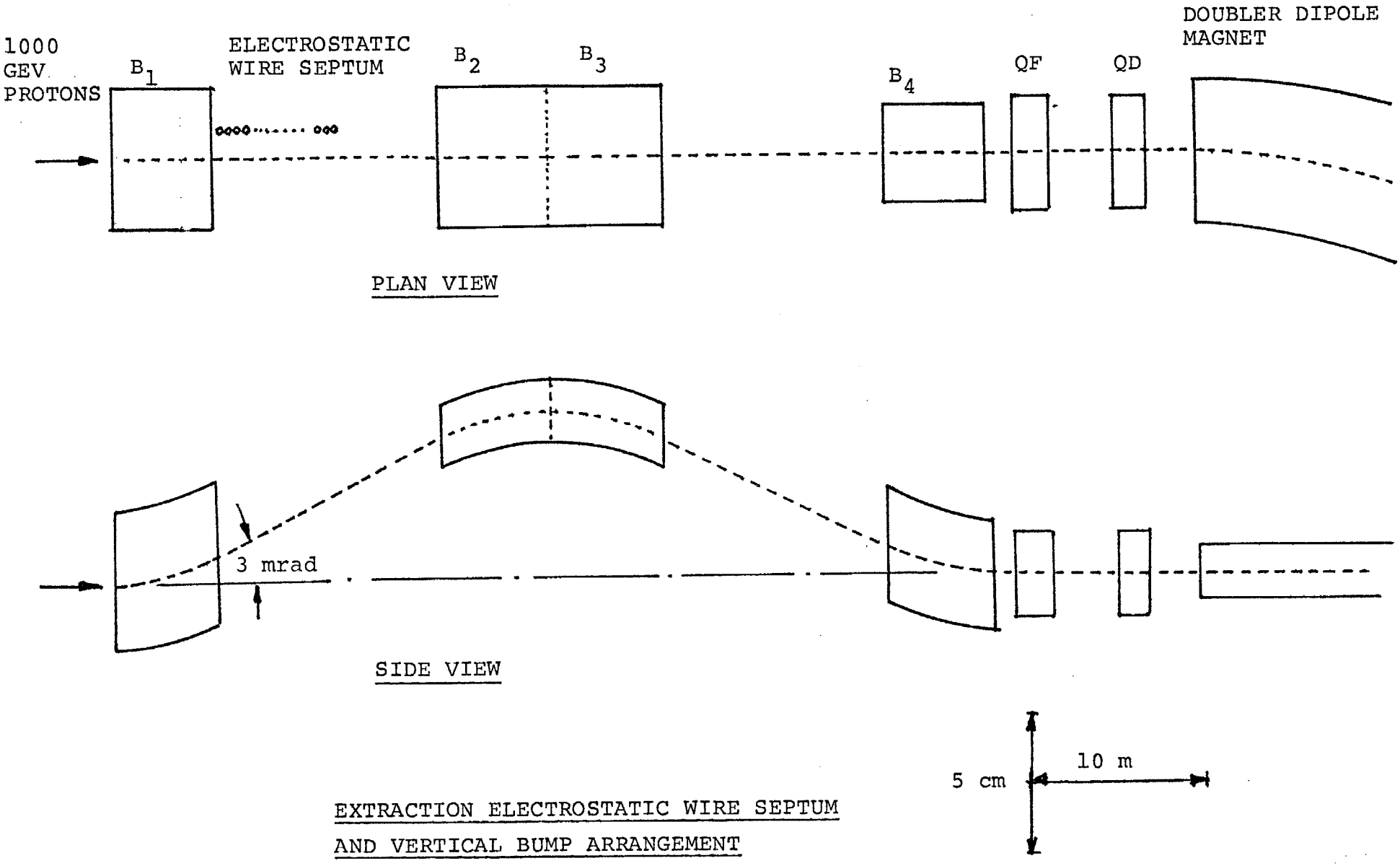

EXTRACTION ELECTROSTATIC WIRE SEPTUM
AND VERTICAL BUMP ARRANGEMENT

Figure 9.

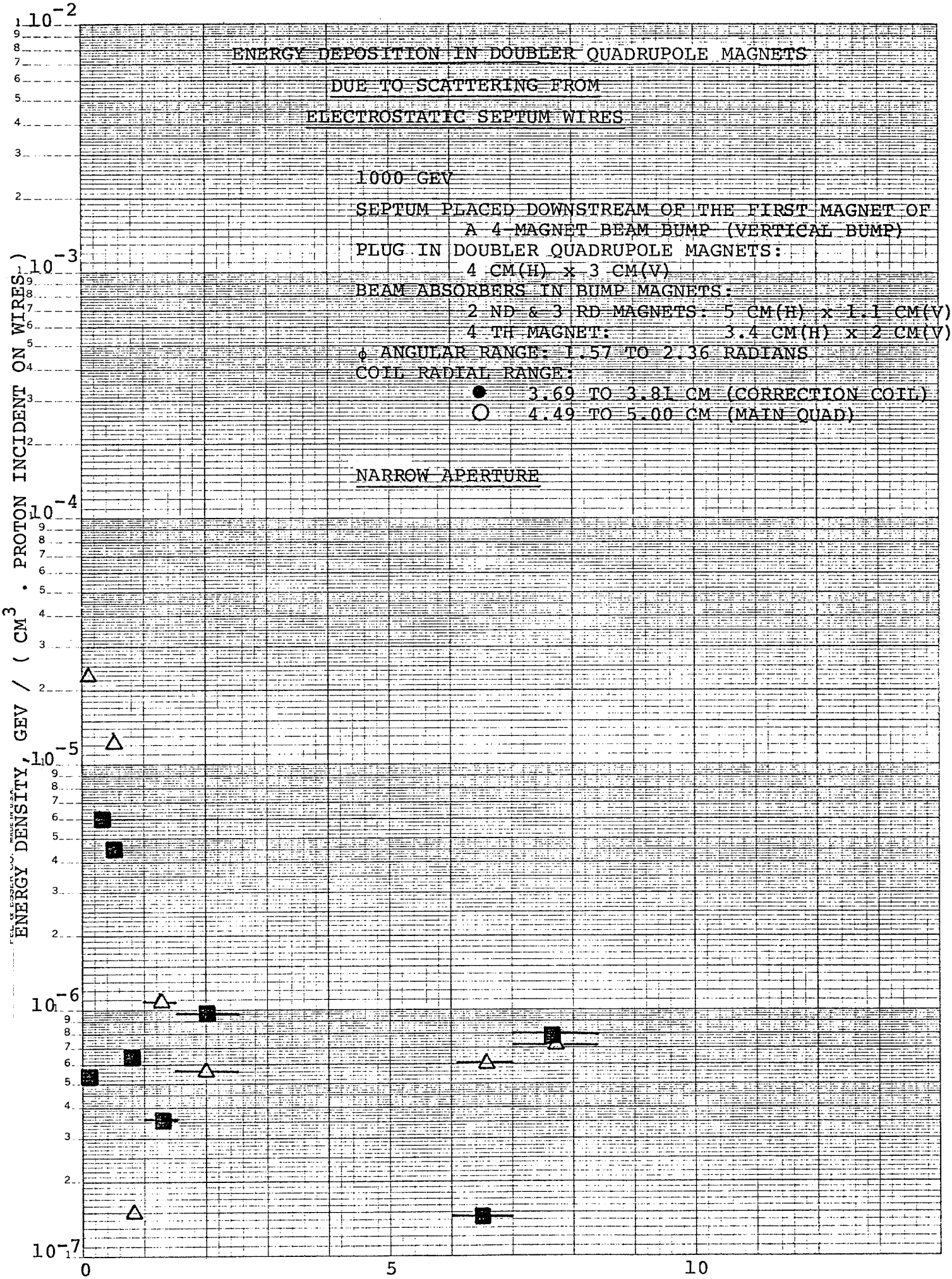
ENERGY DEPOSITION IN DOUBLER QUADRUPOLE MAGNETS
DUE TO SCATTERING FROM
ELECTROSTATIC SEPTUM WIRES
1000 GEV
SEPTUM PLACED DOWNSTREAM OF THE FIRST MAGNET OF A 4-MAGNET BEAM BUMP (VERTICAL BUMP)
PLUG IN DOUBLER QUADRUPOLE MAGNETS:
4 CM(H) x 3 CM(V)
BEAM ABSORBERS IN BUMP MAGNETS:
2 ND & 3 RD MAGNETS: 5 CM(H) x 1.1 CM(V)
4 TH MAGNET: 3.4 CM(H) x 2 CM(V)
φ ANGULAR RANGE: 1.57 TO 2.36 RADIANS
COIL RADIAL RANGE:
● 3.69 TO 3.81 CM (CORRECTION COIL)
○ 4.49 TO 5.00 CM (MAIN QUAD)
NARROW APERTURE
ENERGY DENSITY, GEV / (CM3 · PROTON INCIDENT ON WIRES)
10-2
10-3
10-4
10-5
10-6
10-7
0
5
10
DISTANCE FROM UPSTREAM END OF QUAD STRING (M)

Figure 10.

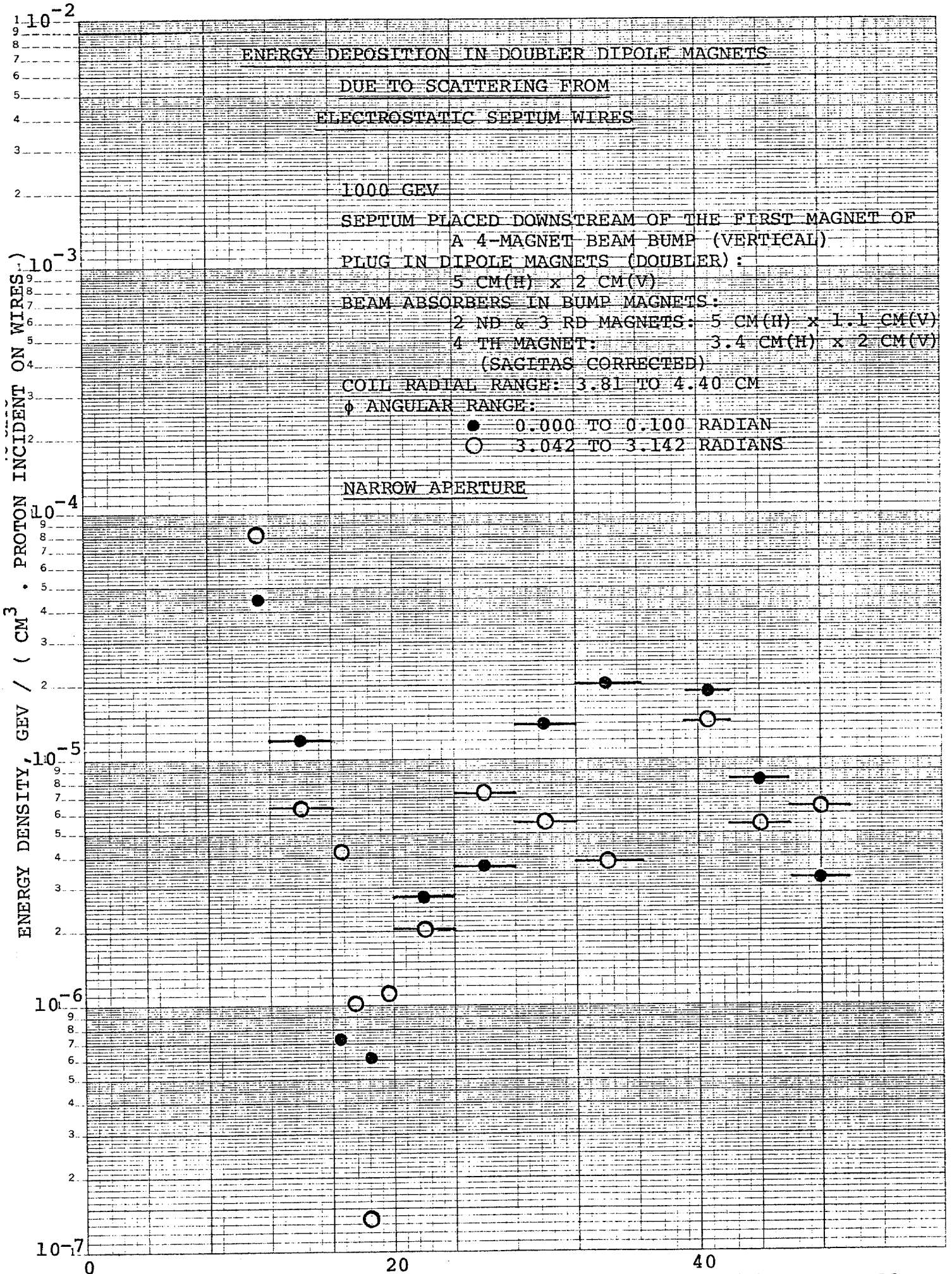
ENERGY DEPOSITION IN DOUBLER DIPOLE MAGNETS
DUE TO SCATTERING FROM
ELECTROSTATIC SEPTUM WIRES
1000 GEV
SEPTUM PLACED DOWNSTREAM OF THE FIRST MAGNET OF
A 4-MAGNET BEAM BUMP (VERTICAL)
PLUG IN DIPOLE MAGNETS (DOUBLER):
5 CM(H) x 2 CM(V)
BEAM ABSORBERS IN BUMP MAGNETS:
2 ND & 3 RD MAGNETS: 5 CM(H) x 1.1 CM(V)
4 TH MAGNET: 3.4 CM(H) x 2 CM(V)
(SAGITAS CORRECTED)
COIL RADIAL RANGE: 3.81 TO 4.40 CM
φ ANGULAR RANGE:
● 0.000 TO 0.100 RADIAN
○ 3.042 TO 3.142 RADIANS
NARROW APERTURE
ENERGY DENSITY, GEV / (CM3 • PROTON INCIDENT ON WIRES)
10-2
10-3
10-4
10-5
10-6
10-7
0
20
40
DISTANCE FROM UPSTREAM END OF QUAD STRING (M)

Figure 11.

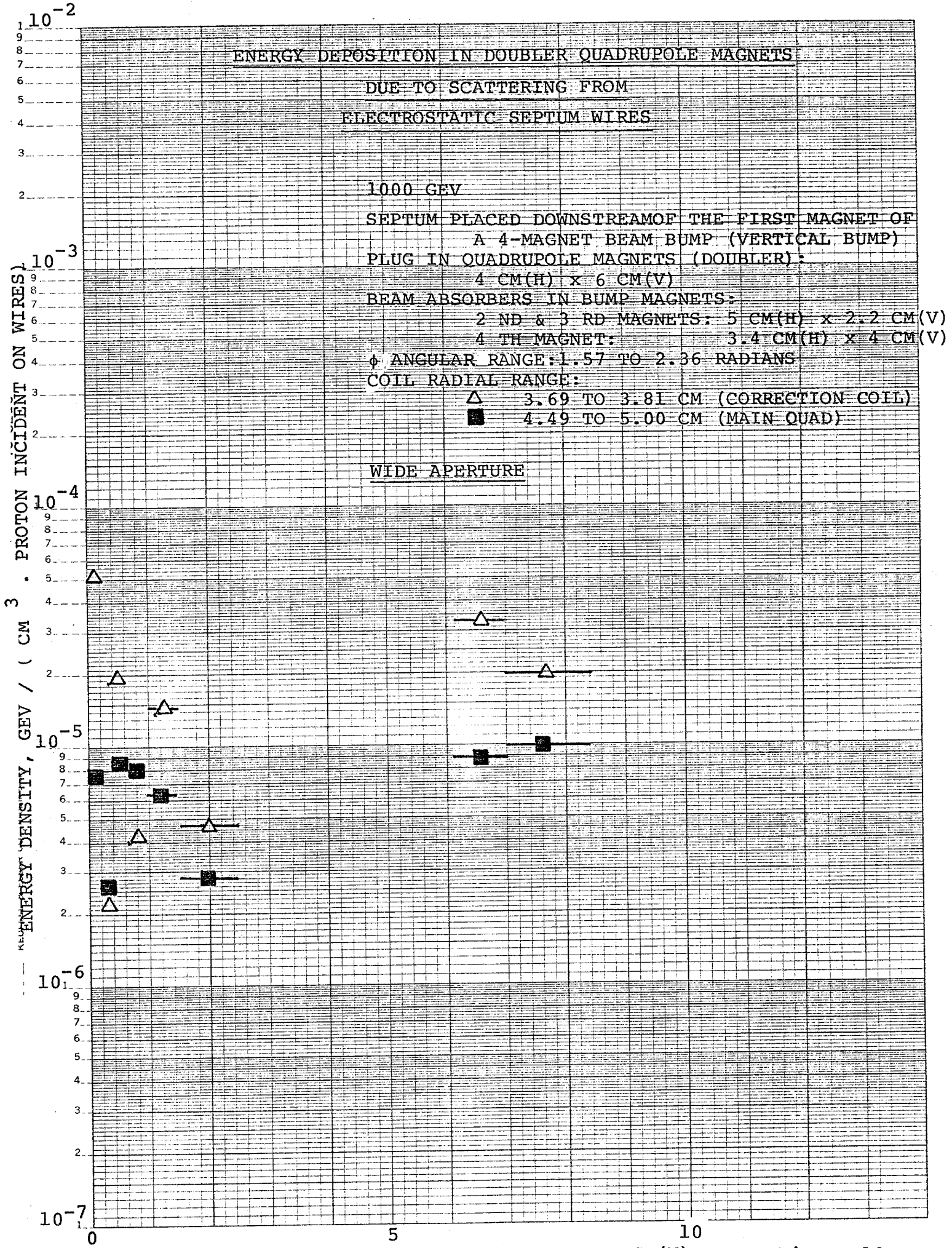
ENERGY DEPOSITION IN DOUBLER QUADRUPOLE MAGNETS
DUE TO SCATTERING FROM
ELECTROSTATIC SEPTUM WIRES
1000 GEV
SEPTUM PLACED DOWNSTREAMOF THE FIRST MAGNET OF
A 4-MAGNET BEAM BUMP (VERTICAL BUMP)
PLUG IN QUADRUPOLE MAGNETS (DOUBLER):
4 CM(H) x 6 CM(V)
BEAM ABSORBERS IN BUMP MAGNETS:
2 ND & 3 RD MAGNETS: 5 CM(H) x 2.2 CM(V)
4 TH MAGNET: 3.4 CM(H) x 4 CM(V)
φ ANGULAR RANGE: 1.57 TO 2.36 RADIANS
COIL RADIAL RANGE:
△ 3.69 TO 3.81 CM (CORRECTION COIL)
■ 4.49 TO 5.00 CM (MAIN QUAD)
WIDE APERTURE
ENERGY DENSITY, GEV / (CM 3 . PROTON INCIDENT ON WIRES)
DISTANCE FROM UPSTREAM END OF QUAD STRING (M)
0
5
10

Figure 12.

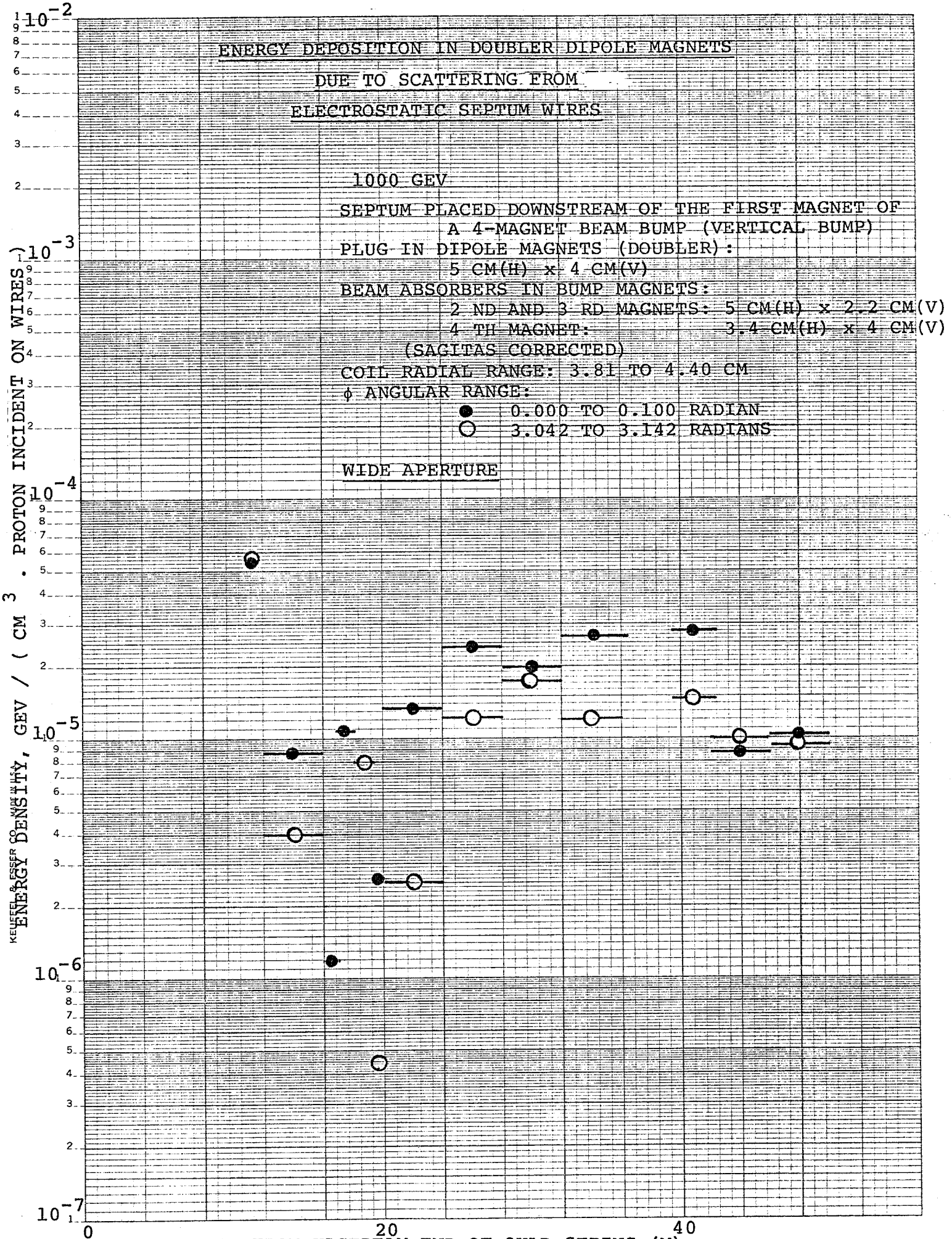
ENERGY DEPOSITION IN DOUBLER DIPOLE MAGNETS
DUE TO SCATTERING FROM
ELECTROSTATIC SEPTUM WIRES
1000 GEV
SEPTUM PLACED DOWNSTREAM OF THE FIRST MAGNET OF
A 4-MAGNET BEAM BUMP (VERTICAL BUMP)
PLUG-IN DIPOLE MAGNETS (DOUBLER):
5 CM(H) x 4 CM(V)
BEAM ABSORBERS IN BUMP MAGNETS:
2 ND AND 3 RD MAGNETS: 5 CM(H) x 2.2 CM(V)
4 TH MAGNET: 3.4 CM(H) x 4 CM(V)
(SAGITAS CORRECTED)
COIL RADIAL RANGE: 3.81 TO 4.40 CM
φ ANGULAR RANGE:
0.000 TO 0.100 RADIAN
3.042 TO 3.142 RADIANS
WIDE APERTURE
ENERGY DENSITY, GEV / (CM 3 . PROTON INCIDENT ON WIRES)
DISTANCE FROM UPSTREAM END OF QUAD STRING (M)
KEUFFEL & ESSER CO.
0
20
40

Figure 13

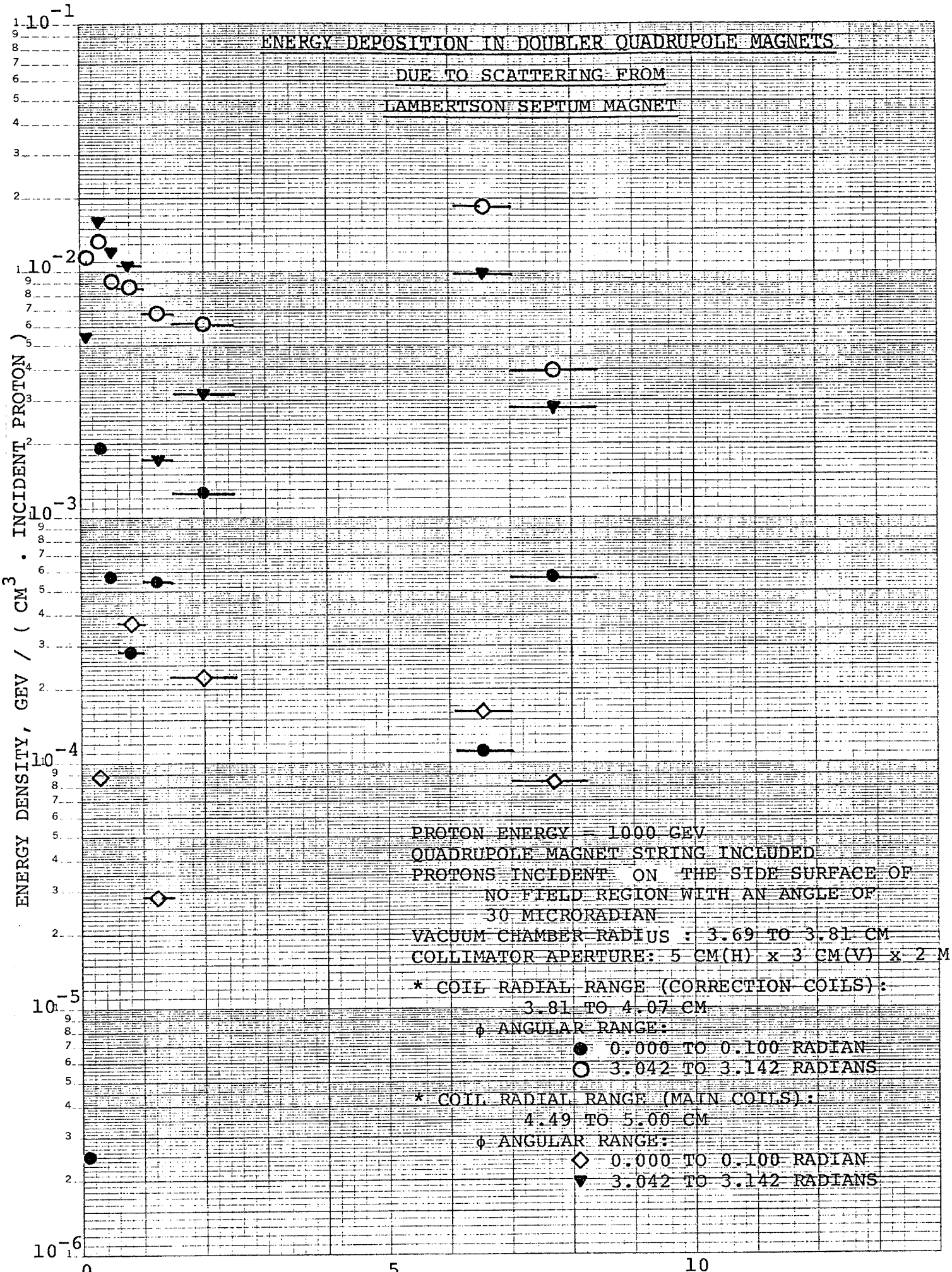
ENERGY DEPOSITION IN DOUBLER QUADRUPOLE MAGNETS
DUE TO SCATTERING FROM
LAMBERTSON SEPTUM MAGNET
ENERGY DENSITY, GEV / (CM3 • INCIDENT PROTON)
PROTON ENERGY = 1000 GEV
QUADRUPOLE MAGNET STRING INCLUDED
PROTONS INCIDENT ON THE SIDE SURFACE OF
NO FIELD REGION WITH AN ANGLE OF
30 MICRORADIAN
VACUUM CHAMBER RADIUS : 3.69 TO 3.81 CM
COLLIMATOR APERTURE: 5 CM(H) x 3 CM(V) x 2 M(L
* COIL RADIAL RANGE (CORRECTION COILS):
3.81 TO 4.07 CM
ϕ ANGULAR RANGE:
0.000 TO 0.100 RADIAN
3.042 TO 3.142 RADIANS
* COIL RADIAL RANGE (MAIN COILS):
4.49 TO 5.00 CM
ϕ ANGULAR RANGE:
0.000 TO 0.100 RADIAN
3.042 TO 3.142 RADIANS
0
5
10
DISTANCE FROM UPSTREAM END OF QUAD STRING (M)

Figure 14.

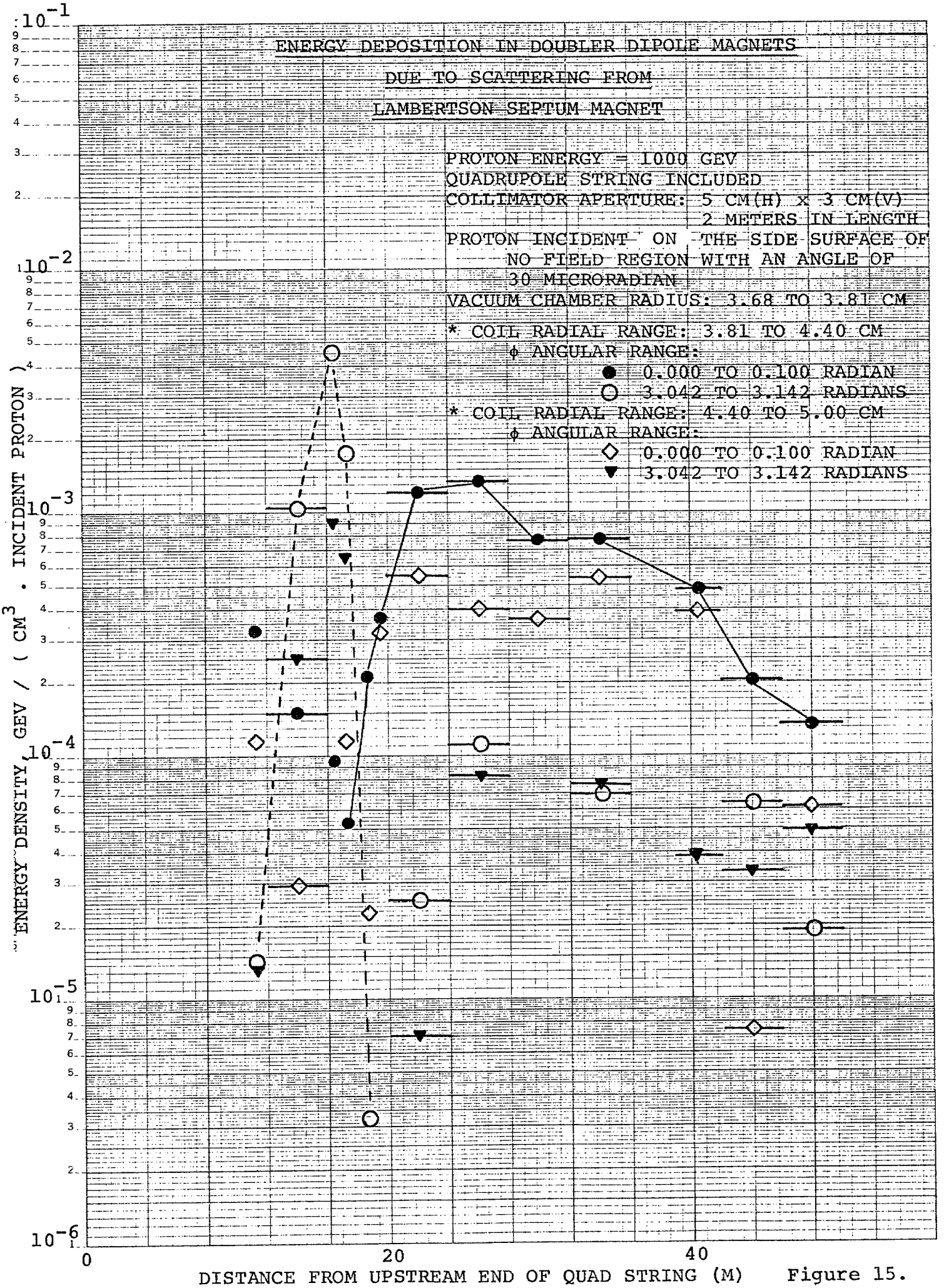
ENERGY DEPOSITION IN DOUBLER DIPOLE MAGNETS
DUE TO SCATTERING FROM
LAMBERTSON SEPTUM MAGNET
PROTON ENERGY = 1000 GEV
QUADRUPOLE STRING INCLUDED
COLLIMATOR APERTURE: 5 CM(H) x 3 CM(V)
2 METERS IN LENGTH
PROTON INCIDENT ON THE SIDE SURFACE OF
NO FIELD REGION WITH AN ANGLE OF
30 MICRORADIAN
VACUUM CHAMBER RADIUS: 3.68 TO 3.81 CM
* COIL RADIAL RANGE: 3.81 TO 4.40 CM
φ ANGULAR RANGE:
0.000 TO 0.100 RADIAN
3.042 TO 3.142 RADIANS
* COIL RADIAL RANGE: 4.40 TO 5.00 CM
φ ANGULAR RANGE:
0.000 TO 0.100 RADIAN
3.042 TO 3.142 RADIANS
ENERGY DENSITY (GEV / (CM3 • INCIDENT PROTON)
10-1
10-2
10-3
10-4
10-5
10-6
0
20
40
DISTANCE FROM UPSTREAM END OF QUAD STRING (M)

Figure 15.

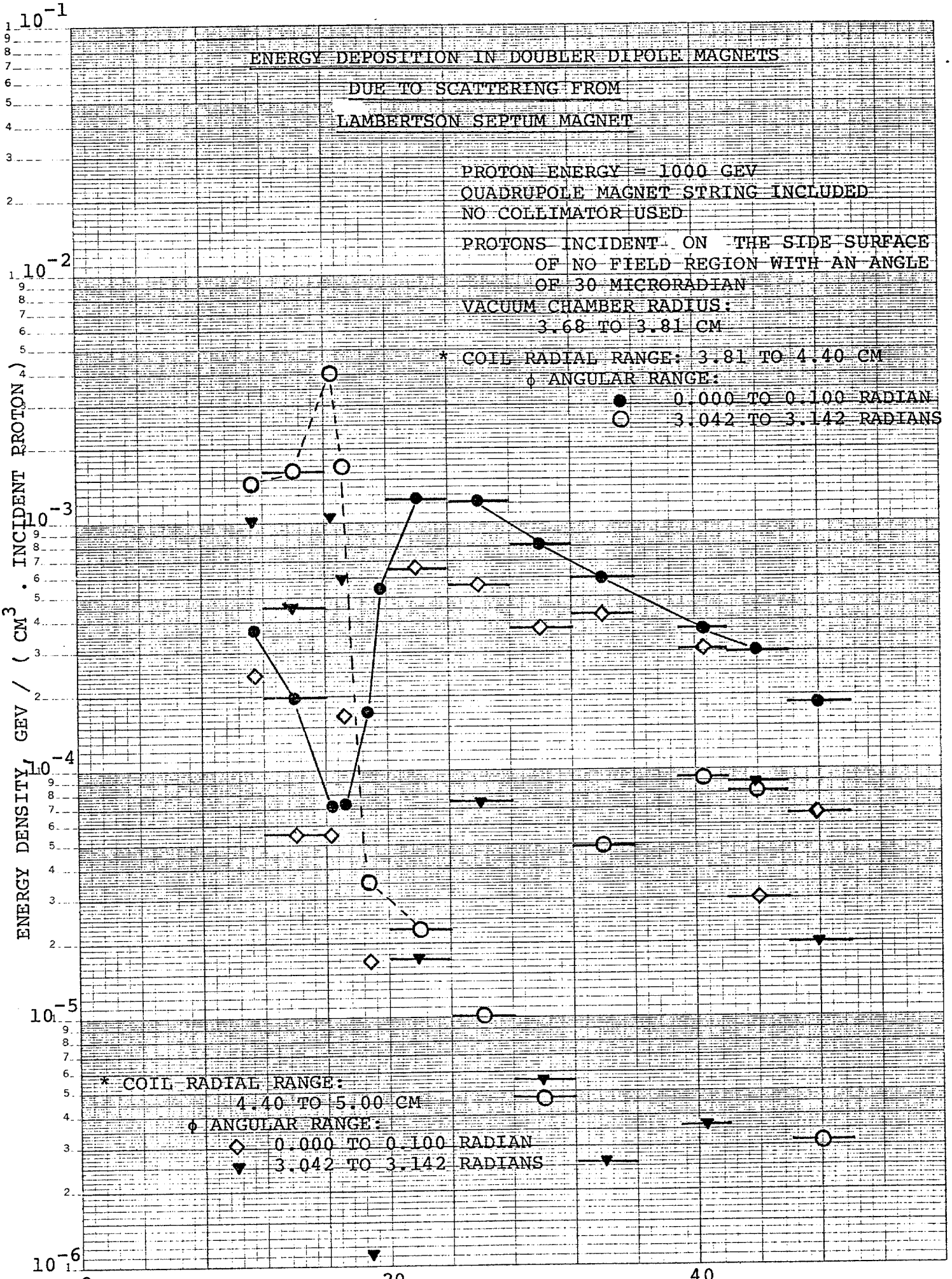
ENERGY DEPOSITION IN DOUBLER DIPOLE MAGNETS
DUE TO SCATTERING FROM
LAMBERTSON SEPTUM MAGNET
PROTON ENERGY = 1000 GEV
QUADRUPOLE MAGNET STRING INCLUDED
NO COLLIMATOR USED
PROTONS INCIDENT ON THE SIDE SURFACE OF NO FIELD REGION WITH AN ANGLE OF 30 MICRORADIAN
VACUUM CHAMBER RADIUS: 3.68 TO 3.81 CM
* COIL RADIAL RANGE: 3.81 TO 4.40 CM
φ ANGULAR RANGE:
0.000 TO 0.100 RADIAN
3.042 TO 3.142 RADIANS
* COIL RADIAL RANGE: 4.40 TO 5.00 CM
φ ANGULAR RANGE:
0.000 TO 0.100 RADIAN
3.042 TO 3.142 RADIANS
ENERGY DENSITY, GEV / (CM3 . INCIDENT PROTON)
DISTANCE FROM UPSTREAM END OF QUAD STRING
0
20
40

Figure 16.

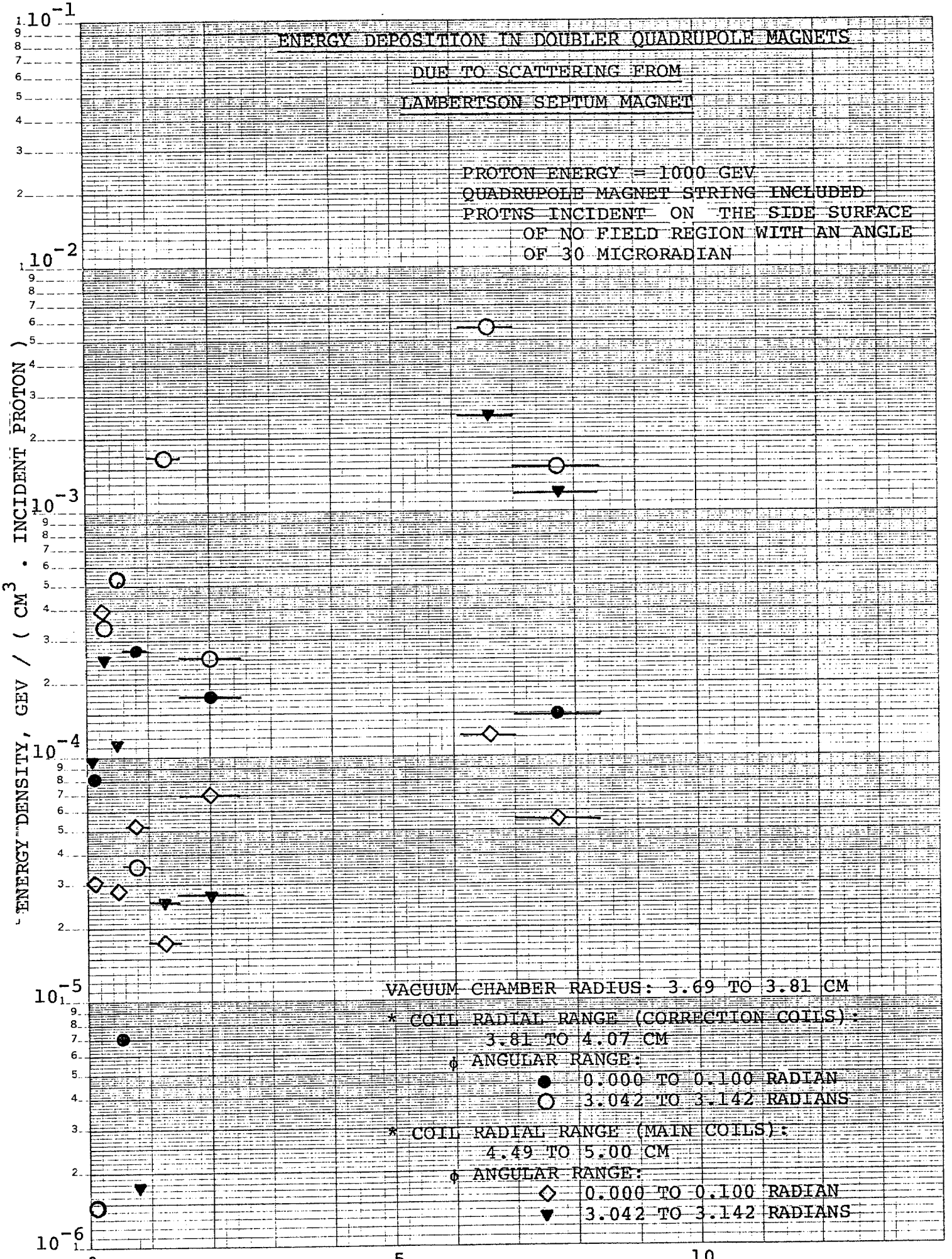
ENERGY DEPOSITION IN DOUBLER QUADRUPOLE MAGNETS
DUE TO SCATTERING FROM
LAMBERTSON SEPTUM MAGNET
PROTON ENERGY = 1000 GEV
QUADRUPOLE MAGNET STRING INCLUDED
PROTNS INCIDENT ON THE SIDE SURFACE
OF NO FIELD REGION WITH AN ANGLE
OF 30 MICRORADIAN
"ENERGY"DENSITY, GEV / (CM3 • INCIDENT PROTON)
VACUUM CHAMBER RADIUS: 3.69 TO 3.81 CM
* COIL RADIAL RANGE (CORRECTION COILS):
3.81 TO 4.07 CM
ϕ ANGULAR RANGE:
0.000 TO 0.100 RADIAN
3.042 TO 3.142 RADIANS
* COIL RADIAL RANGE (MAIN COILS):
4.49 TO 5.00 CM
ϕ ANGULAR RANGE:
0.000 TO 0.100 RADIAN
3.042 TO 3.142 RADIANS
DISTANCE FROM UPSTREAM END OF QUAD STRING (M)

Figure 17.

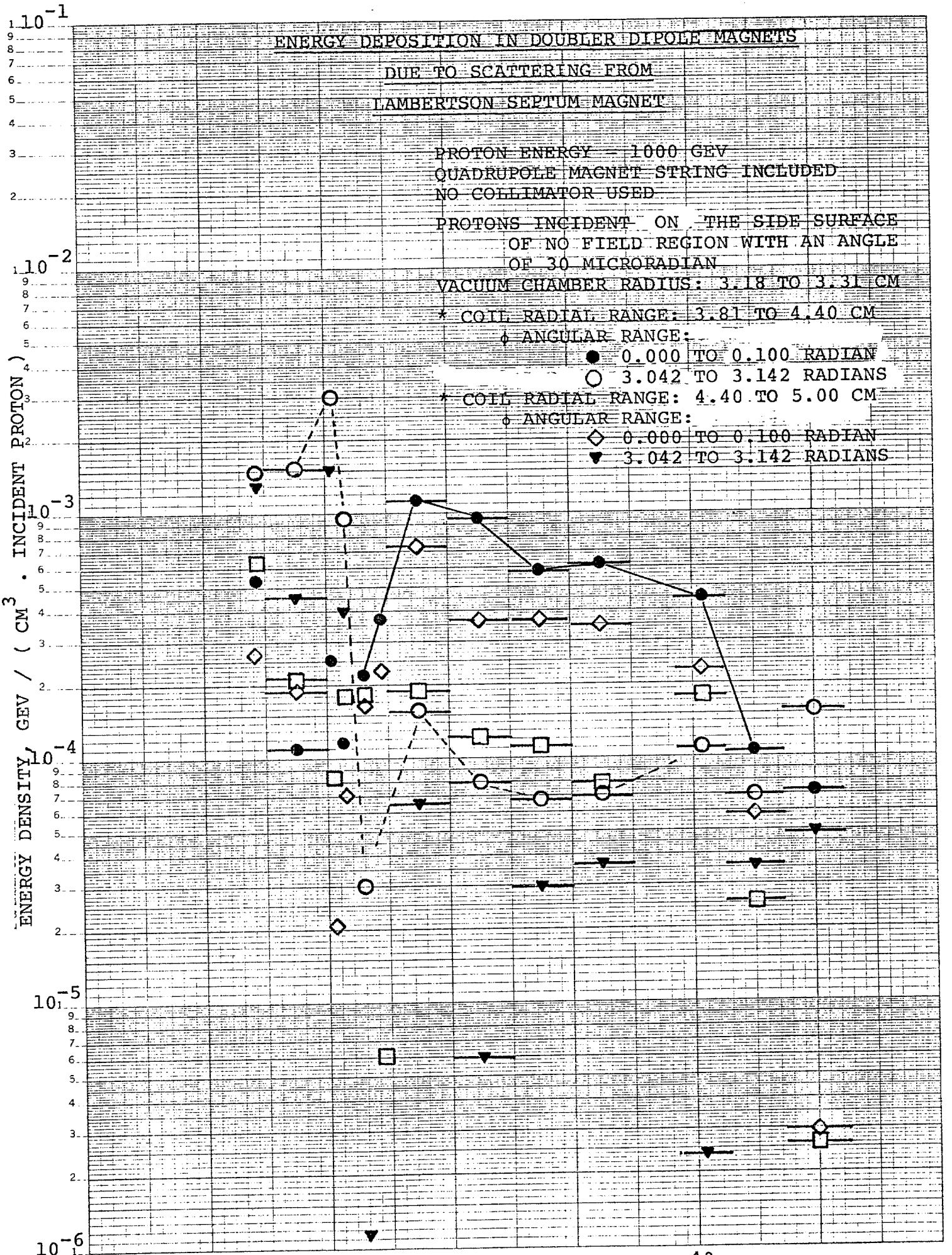
ENERGY DEPOSITION IN DOUBLER DIPOLE MAGNETS
DUE TO SCATTERING FROM
LAMBERTSON SEPTUM MAGNET
PROTON ENERGY = 1000 GEV
QUADRUPOLE MAGNET STRING INCLUDED
NO COLLIMATOR USED
PROTONS INCIDENT ON THE SIDE SURFACE OF NO FIELD REGION WITH AN ANGLE OF 30 MICRORADIAN
VACUUM CHAMBER RADIUS: 3.18 TO 3.31 CM
* COIL RADIAL RANGE: 3.81 TO 4.40 CM
φ ANGULAR RANGE:
● 0.000 TO 0.100 RADIAN
○ 3.042 TO 3.142 RADIANS
* COIL RADIAL RANGE: 4.40 TO 5.00 CM
φ ANGULAR RANGE:
◇ 0.000 TO 0.100 RADIAN
▼ 3.042 TO 3.142 RADIANS
ENERGY DENSITY, GEV / (CM3 • INCIDENT PROTON)
10-1
10-2
10-3
10-4
10-5
10-6
0
20
40
DISTANCE FROM UPSTREAM END OF QUAD STRING (M)

Figure 18.

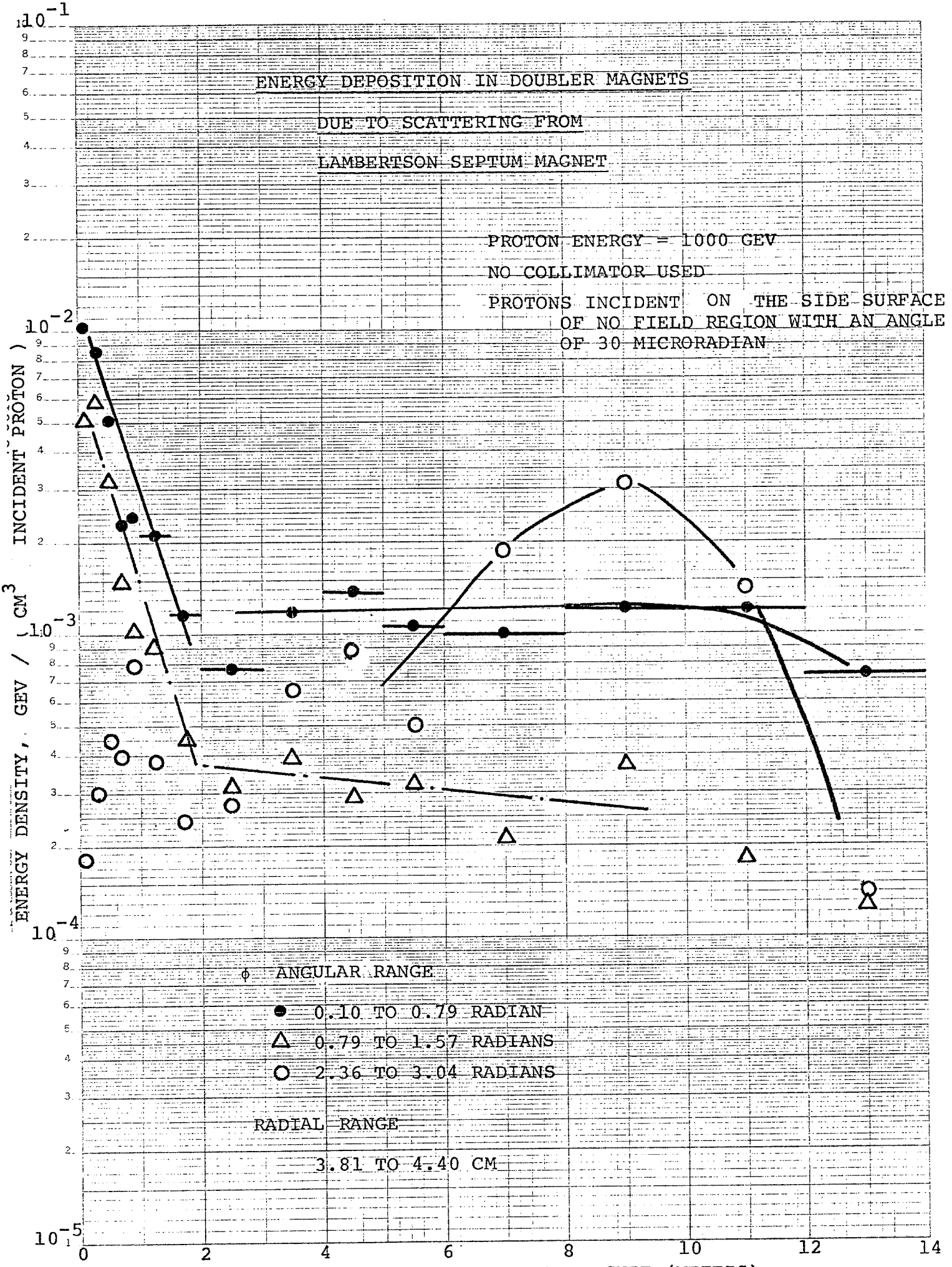
ENERGY DEPOSITION IN DOUBLER MAGNETS
DUE TO SCATTERING FROM
LAMBERTSON SEPTUM MAGNET
PROTON ENERGY = 1000 GEV
NO COLLIMATOR USED
PROTONS INCIDENT ON THE SIDE SURFACE OF NO FIELD REGION WITH AN ANGLE OF 30 MICRORADIAN
ENERGY DENSITY, GEV / (CM3 INCIDENT PROTON)
10-1
10-2
10-3
10-4
10-5
ϕ ANGULAR RANGE
0.10 TO 0.79 RADIAN
0.79 TO 1.57 RADIANS
2.36 TO 3.04 RADIANS
RADIAL RANGE
3.81 TO 4.40 CM
0
2
4
6
8
10
12
14
DISTANCE FROM UPSTREAM END OF MAGNET (METERS)

Figure 19.

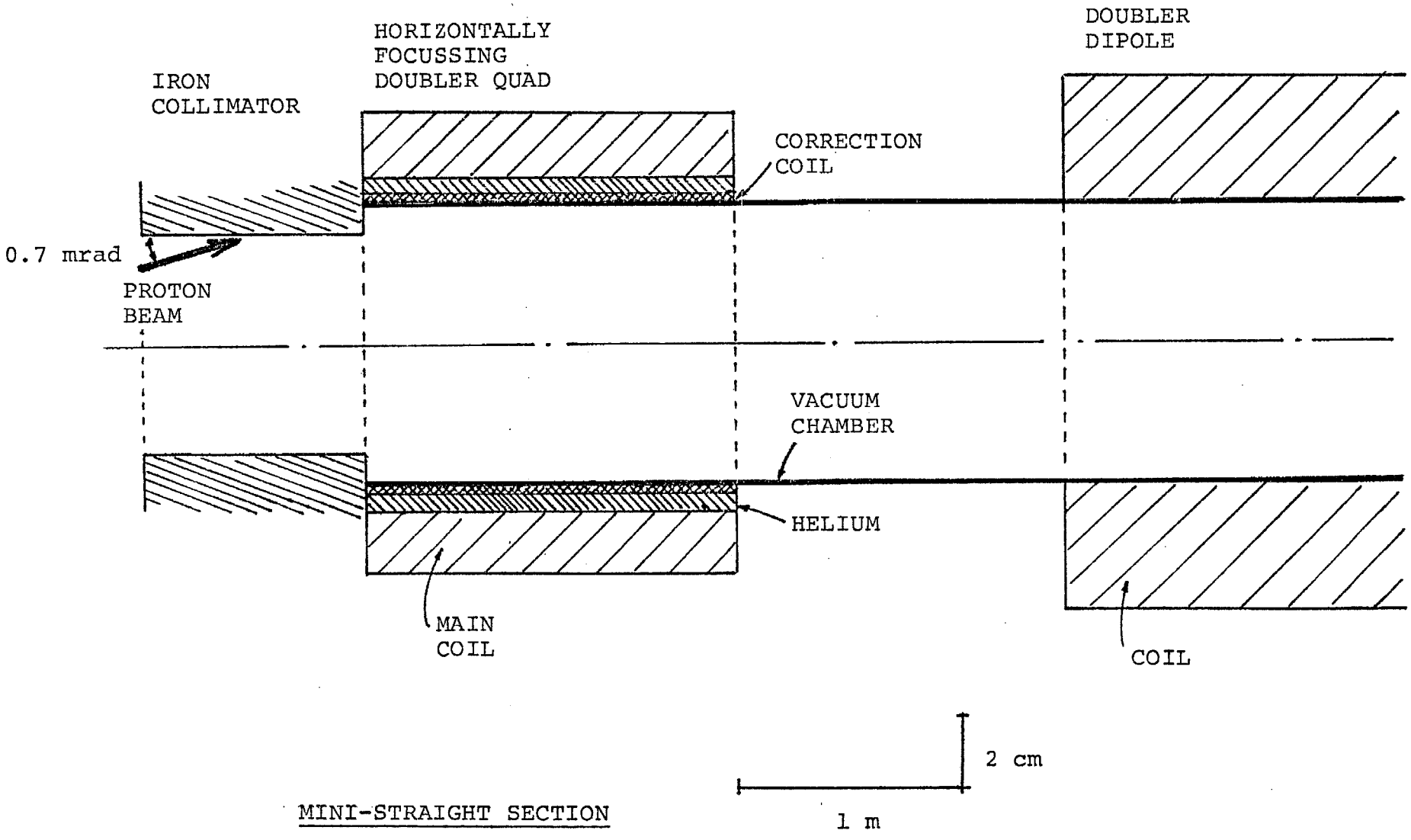
HORIZONTALLY
FOCUSSING
DOUBLER QUAD
DOUBLER
DIPOLE
IRON
COLLIMATOR
CORRECTION
COIL
0.7 mrad
PROTON
BEAM
VACUUM
CHAMBER
HELIUM
MAIN
COIL
COIL
2 cm
1 m
MINI-STRAIGHT SECTION

Figure 20.

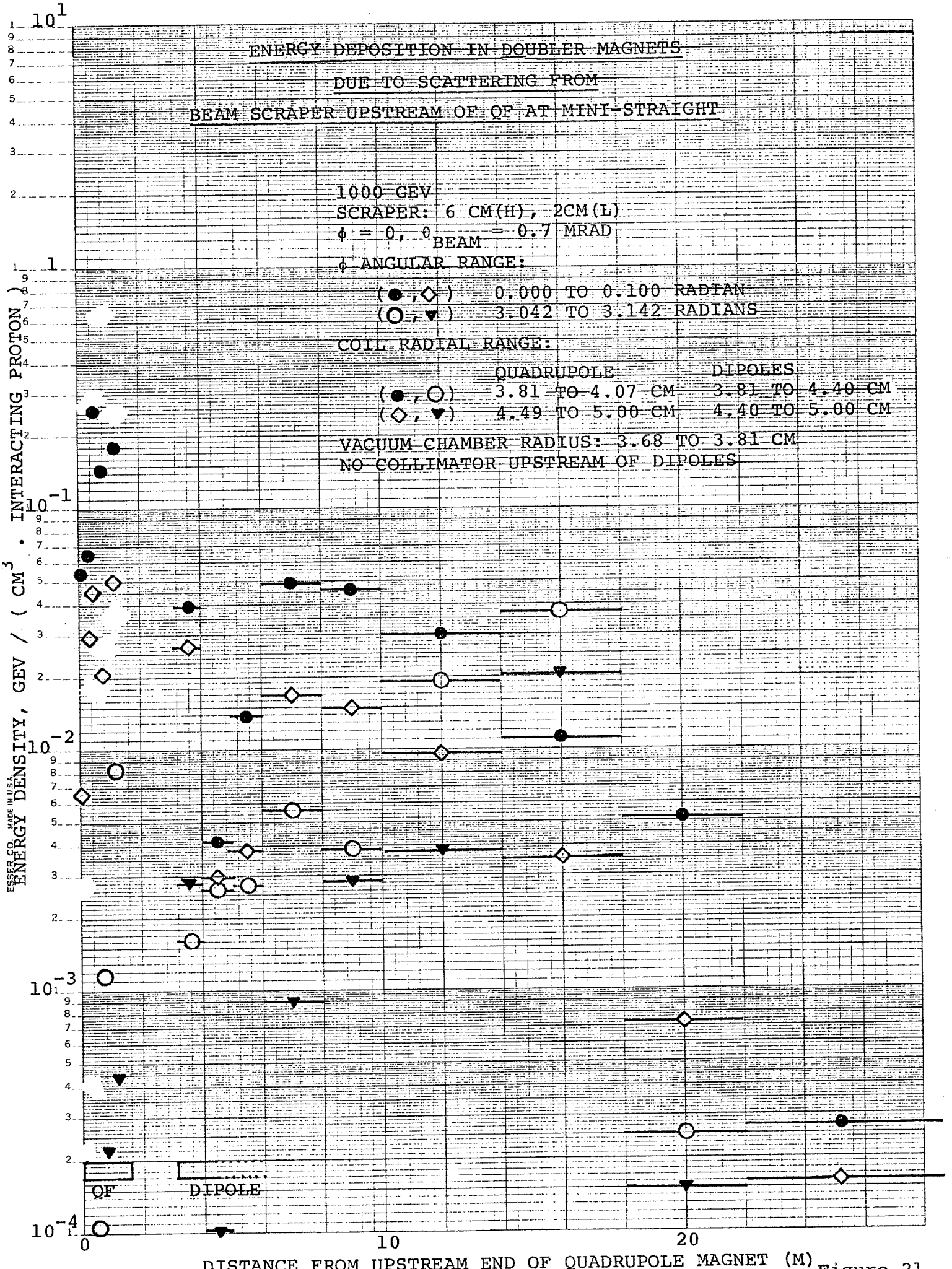
ENERGY DEPOSITION IN DOUBLER MAGNETS
DUE TO SCATTERING FROM
BEAM SCRAPER UPSTREAM OF QF AT MINI-STRAIGHT
1000 GEV
SCRAPER: 6 CM(H), 2CM(L)
$\phi = 0$, $\theta_{BEAM} = 0.7$ MRAD
ϕ ANGULAR RANGE:
(●, ◇) 0.000 TO 0.100 RADIAN
(○, ▼) 3.042 TO 3.142 RADIANS
COIL RADIAL RANGE:
QUADRUPOLE DIPOLES
(●, ○) 3.81 TO 4.07 CM 3.81 TO 4.40 CM
(◇, ▼) 4.49 TO 5.00 CM 4.40 TO 5.00 CM
VACUUM CHAMBER RADIUS: 3.68 TO 3.81 CM
NO COLLIMATOR UPSTREAM OF DIPOLES
ENERGY DENSITY, GEV / (CM^3 · INTERACTING PROTON)
10^1
1
10^{-1}
10^{-2}
10^{-3}
10^{-4}
QF
DIPOLE
0
10
20
DISTANCE FROM UPSTREAM END OF QUADRUPOLE MAGNET (M)
ESSER CO. MADE IN U.S.A.

Figure 21.

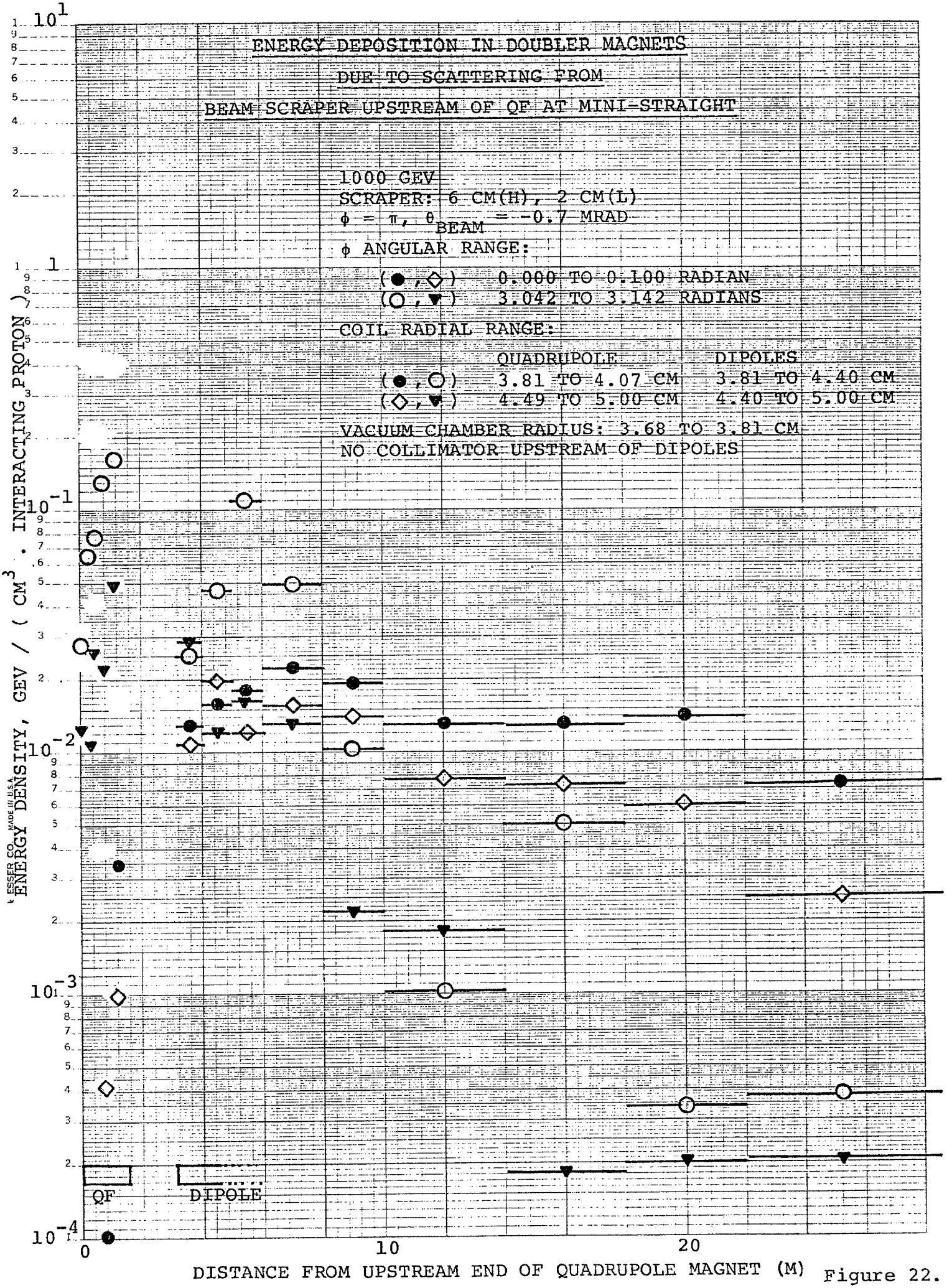
ENERGY DEPOSITION IN DOUBLER MAGNETS
DUE TO SCATTERING FROM
BEAM SCRAPER UPSTREAM OF QF AT MINI-STRAIGHT
1000 GEV
SCRAPER: 6 CM(H), 2 CM(L)
φ = π, θ BEAM = -0.7 MRAD
φ ANGULAR RANGE:
(●, ◇) 0.000 TO 0.100 RADIAN
(○, ▼) 3.042 TO 3.142 RADIANS
COIL RADIAL RANGE:
QUADRUPOLE DIPOLES
(●, ○) 3.81 TO 4.07 CM 3.81 TO 4.40 CM
(◇, ▼) 4.49 TO 5.00 CM 4.40 TO 5.00 CM
VACUUM CHAMBER RADIUS: 3.68 TO 3.81 CM
NO COLLIMATOR UPSTREAM OF DIPOLES
ENERGY DENSITY, GEV / (CM3 · INTERACTING PROTON)
QF
DIPOLE
0
10
20
DISTANCE FROM UPSTREAM END OF QUADRUPOLE MAGNET (M)

Figure 22.

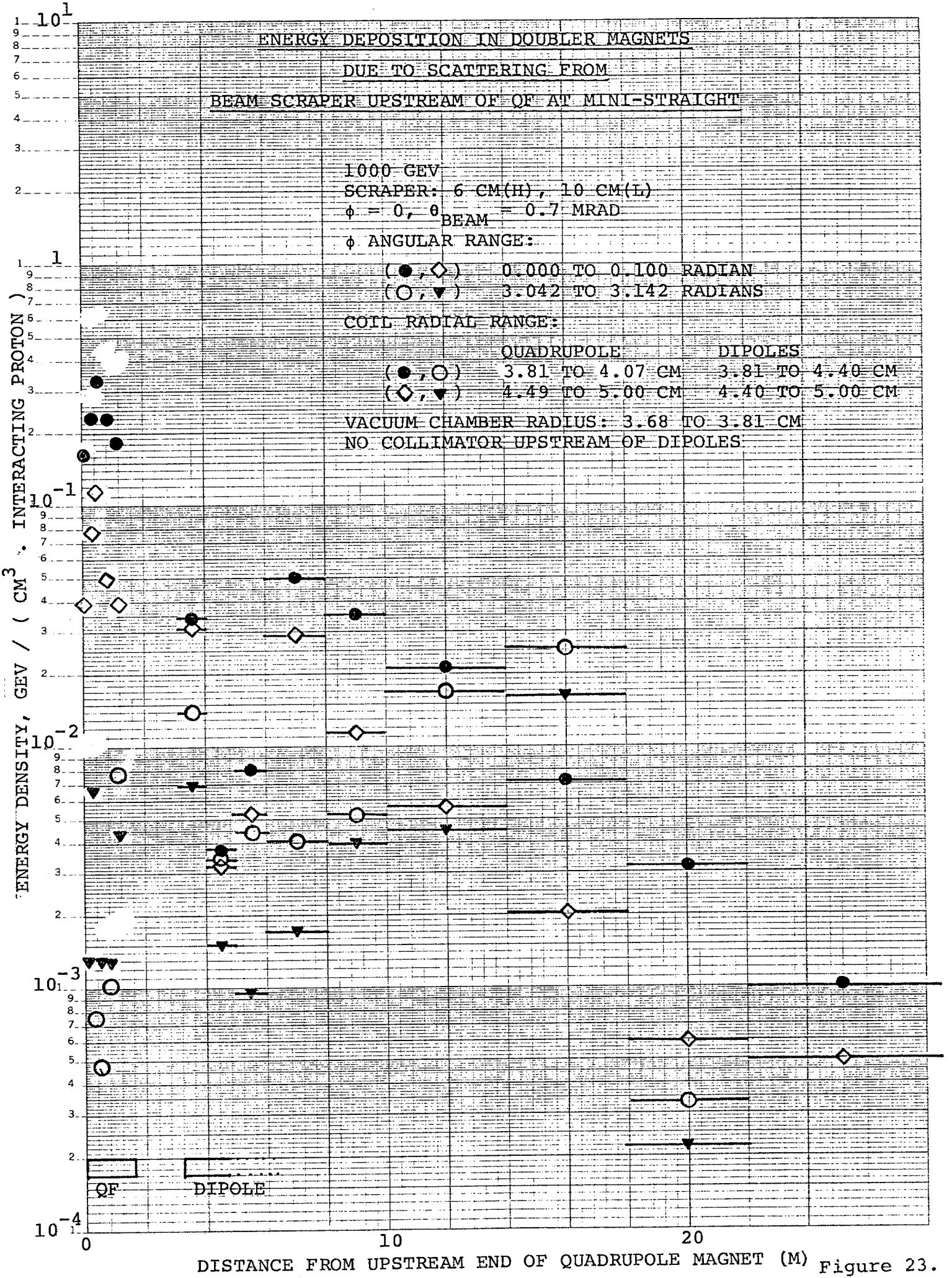
ENERGY DEPOSITION IN DOUBLER MAGNETS
DUE TO SCATTERING FROM
BEAM SCRAPER UPSTREAM OF QF AT MINI-STRAIGHT
1000 GEV
SCRAPER: 6 CM(H), 10 CM(L)
ϕ = 0, θ_{BEAM} = 0.7 MRAD
ϕ ANGULAR RANGE:
(●, ◇) 0.000 TO 0.100 RADIAN
(○, ▼) 3.042 TO 3.142 RADIANS
COIL RADIAL RANGE:
QUADRUPOLE DIPOLES
(●, ○) 3.81 TO 4.07 CM 3.81 TO 4.40 CM
(◇, ▼) 4.49 TO 5.00 CM 4.40 TO 5.00 CM
VACUUM CHAMBER RADIUS: 3.68 TO 3.81 CM
NO COLLIMATOR UPSTREAM OF DIPOLES
ENERGY DENSITY, GEV / (CM^3 . INTERACTING PROTON)
10^{1}
1
10^{-1}
10^{-2}
10^{-3}
10^{-4}
QF
DIPOLE
0
10
20
DISTANCE FROM UPSTREAM END OF QUADRUPOLE MAGNET (M)

Figure 23.

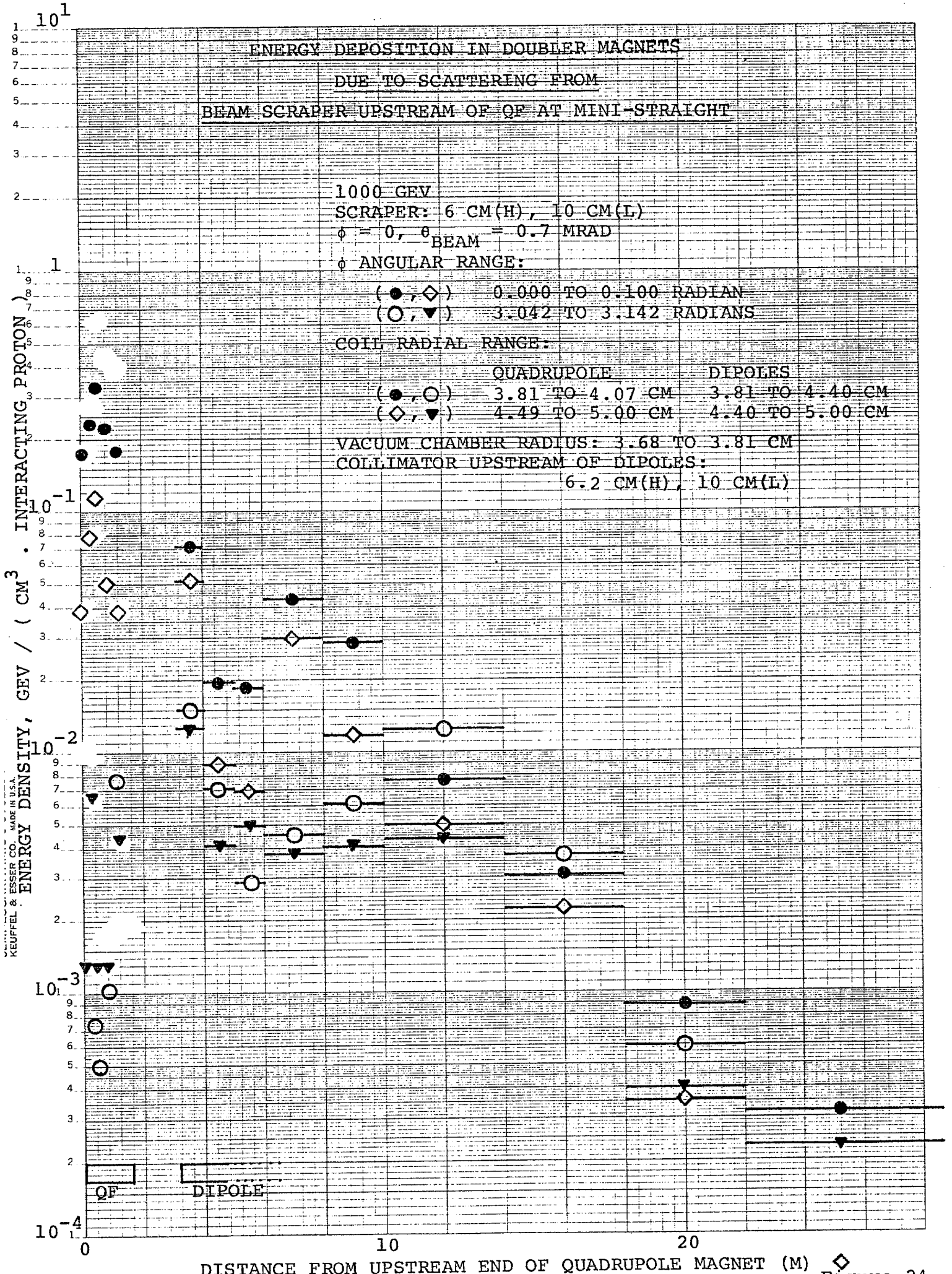
ENERGY DEPOSITION IN DOUBLER MAGNETS
DUE TO SCATTERING FROM
BEAM SCRAPER UPSTREAM OF QF AT MINI-STRAIGHT
1000 GEV
SCRAPER: 6 CM(H), 10 CM(L)
φ = 0, θBEAM = 0.7 MRAD
φ ANGULAR RANGE:
(●,◇) 0.000 TO 0.100 RADIAN
(○,▼) 3.042 TO 3.142 RADIANS
COIL RADIAL RANGE:
QUADRUPOLE DIPOLES
(●,○) 3.81 TO 4.07 CM 3.81 TO 4.40 CM
(◇,▼) 4.49 TO 5.00 CM 4.40 TO 5.00 CM
VACUUM CHAMBER RADIUS: 3.68 TO 3.81 CM
COLLIMATOR UPSTREAM OF DIPOLES:
6.2 CM(H), 10 CM(L)
ENERGY DENSITY, GEV / (CM3 . INTERACTING PROTON)
QF
DIPOLE
0
10
20
DISTANCE FROM UPSTREAM END OF QUADRUPOLE MAGNET (M)
KEUFFEL & ESSER CO. MADE IN U.S.A.

Figure 24.

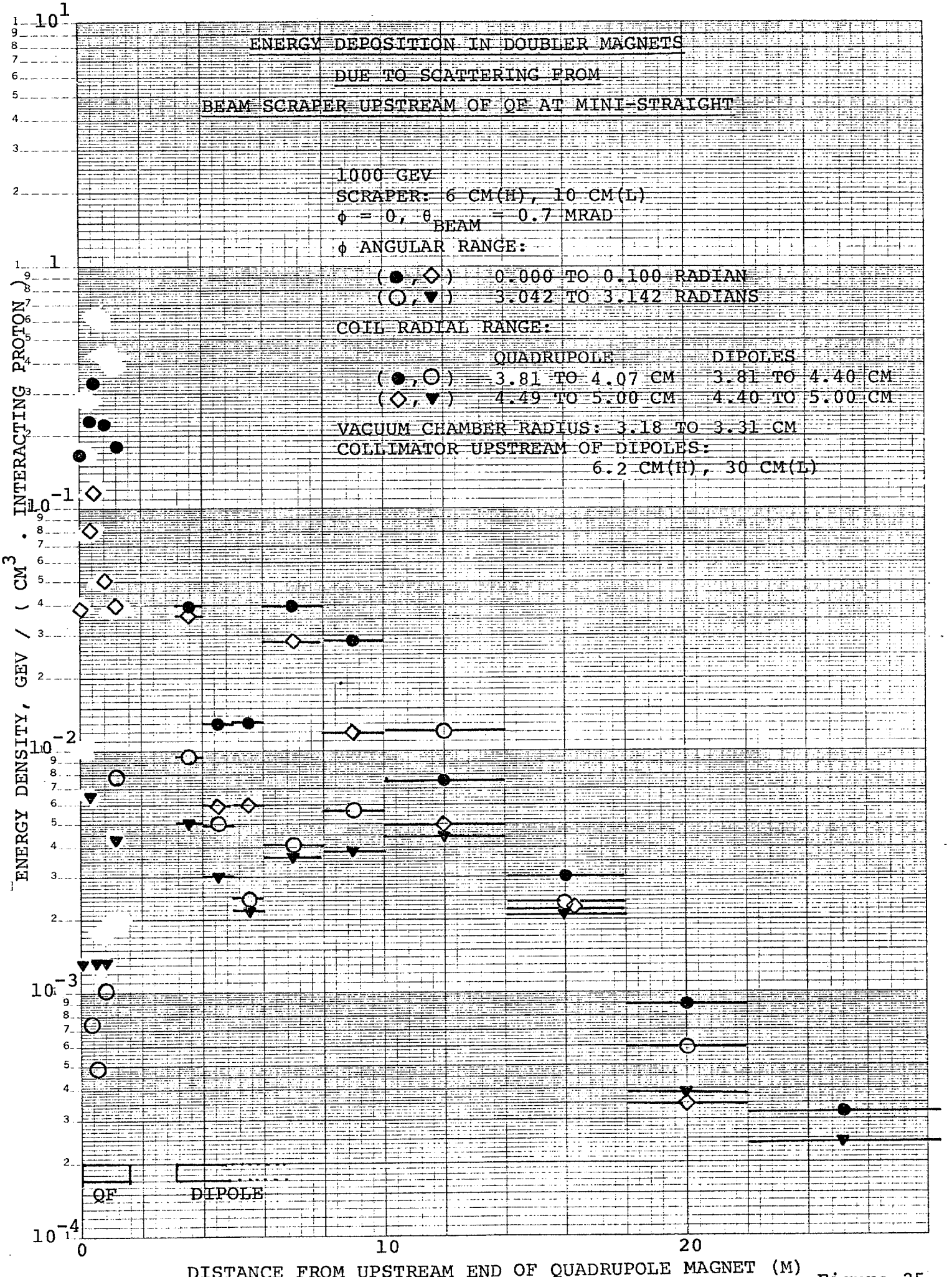
ENERGY DEPOSITION IN DOUBLER MAGNETS
DUE TO SCATTERING FROM
BEAM SCRAPER UPSTREAM OF QF AT MINI-STRAIGHT
1000 GEV
SCRAPER: 6 CM(H), 10 CM(L)
ϕ = 0, θ_{BEAM} = 0.7 MRAD
ϕ ANGULAR RANGE:
(●,◇) 0.000 TO 0.100 RADIAN
(○,▼) 3.042 TO 3.142 RADIANS
COIL RADIAL RANGE:
QUADRUPOLE DIPOLES
(●,○) 3.81 TO 4.07 CM 3.81 TO 4.40 CM
(◇,▼) 4.49 TO 5.00 CM 4.40 TO 5.00 CM
VACUUM CHAMBER RADIUS: 3.18 TO 3.31 CM
COLLIMATOR UPSTREAM OF DIPOLES:
6.2 CM(H), 30 CM(L)
ENERGY DENSITY, GEV / (CM^3 . INTERACTING PROTON)
10^{1}
1
10^{-1}
10^{-2}
10^{-3}
10^{-4}
QF
DIPOLE
0
10
20
DISTANCE FROM UPSTREAM END OF QUADRUPOLE MAGNET (M)

Figure 25.

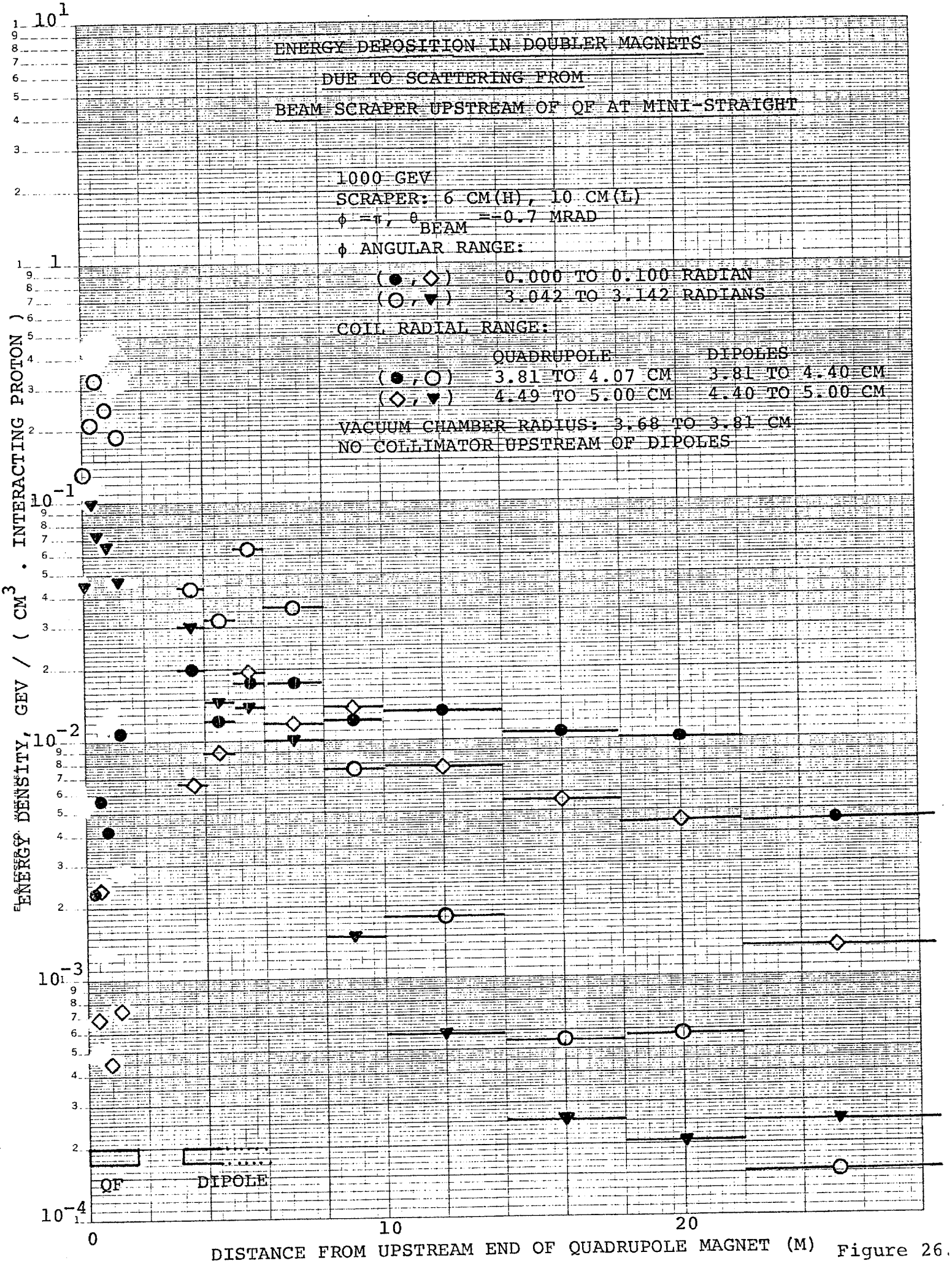
ENERGY DEPOSITION IN DOUBLER MAGNETS
DUE TO SCATTERING FROM
BEAM SCRAPER UPSTREAM OF QF AT MINI-STRAIGHT
1000 GEV
SCRAPER: 6 CM(H), 10 CM(L)
$\phi = \pi$, $\theta_{BEAM} = -0.7$ MRAD
ϕ ANGULAR RANGE:
(●, ◇) 0.000 TO 0.100 RADIAN
(○, ▼) 3.042 TO 3.142 RADIANS
COIL RADIAL RANGE:
QUADRUPOLE DIPOLES
(●, ○) 3.81 TO 4.07 CM 3.81 TO 4.40 CM
(◇, ▼) 4.49 TO 5.00 CM 4.40 TO 5.00 CM
VACUUM CHAMBER RADIUS: 3.68 TO 3.81 CM
NO COLLIMATOR UPSTREAM OF DIPOLES
ENERGY DENSITY, GEV / (CM^3 · INTERACTING PROTON)
10^1
1
10^{-1}
10^{-2}
10^{-3}
10^{-4}
QF
DIPOLE
0
10
20
DISTANCE FROM UPSTREAM END OF QUADRUPOLE MAGNET (M)

Figure 26.

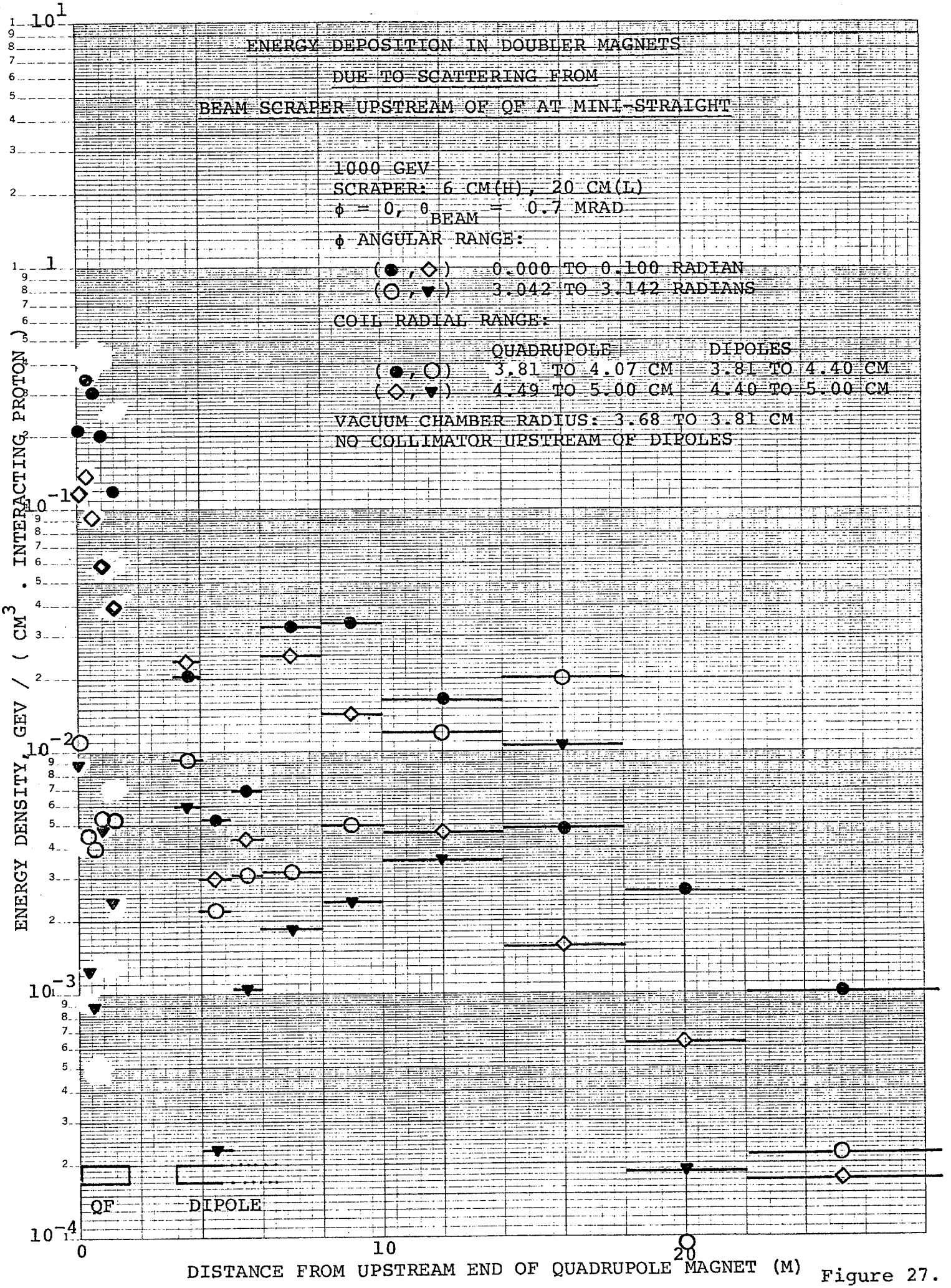
ENERGY DEPOSITION IN DOUBLER MAGNETS
DUE TO SCATTERING FROM
BEAM SCRAPER UPSTREAM OF QF AT MINI-STRAIGHT
1000 GEV
SCRAPER: 6 CM(H), 20 CM(L)
φ = 0, θ BEAM = 0.7 MRAD
φ ANGULAR RANGE:
(●, ◇) 0.000 TO 0.100 RADIAN
(○, ▼) 3.042 TO 3.142 RADIANS
COIL RADIAL RANGE:
QUADRUPOLE DIPOLES
(●, ○) 3.81 TO 4.07 CM 3.81 TO 4.40 CM
(◇, ▼) 4.49 TO 5.00 CM 4.40 TO 5.00 CM
VACUUM CHAMBER RADIUS: 3.68 TO 3.81 CM
NO COLLIMATOR UPSTREAM OF DIPOLES
ENERGY DENSITY, GEV / (CM3 . INTERACTING PROTON)
QF
DIPOLE
0
10
20
DISTANCE FROM UPSTREAM END OF QUADRUPOLE MAGNET (M)

Figure 27.

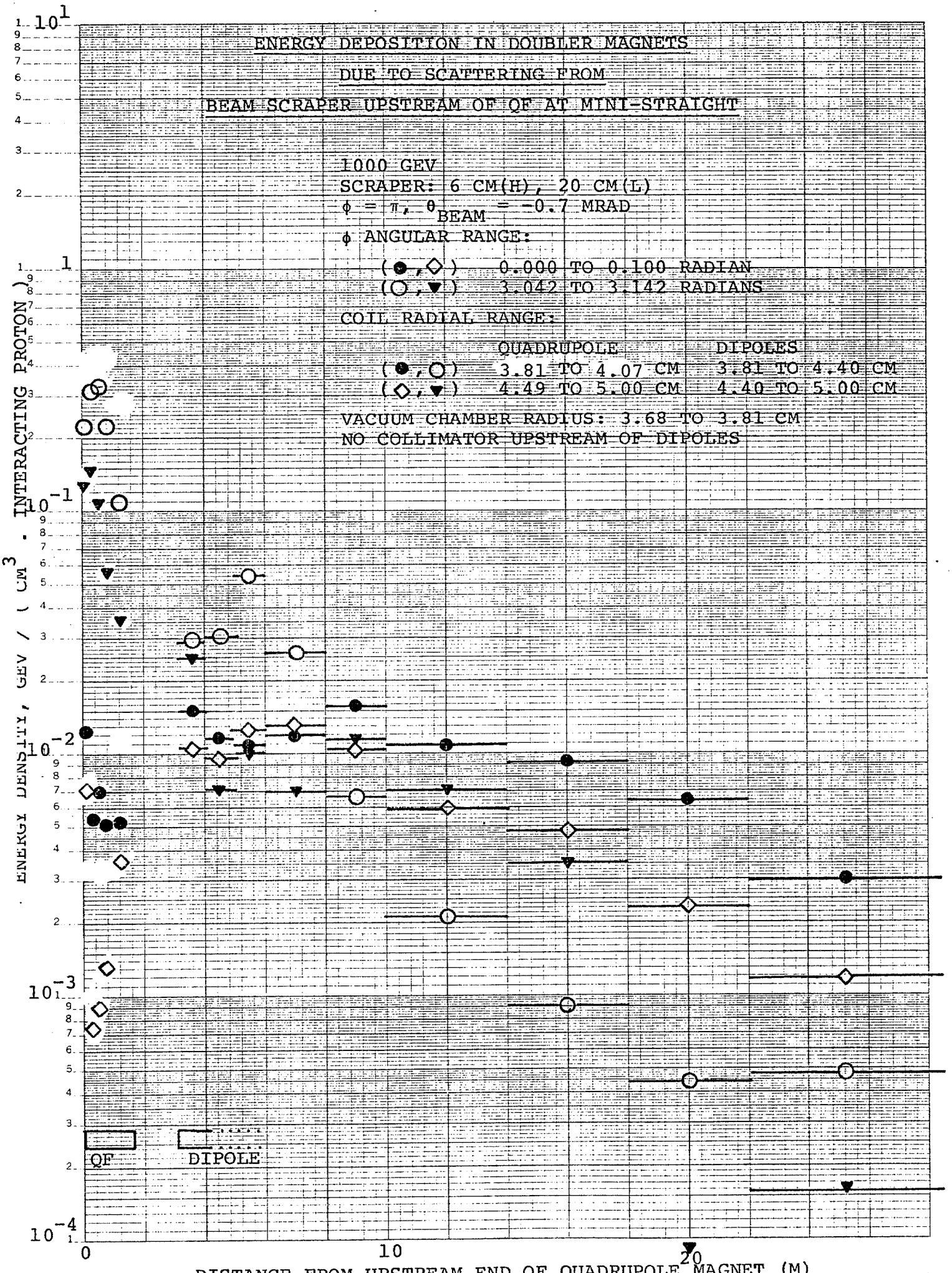
ENERGY DEPOSITION IN DOUBLER MAGNETS
DUE TO SCATTERING FROM
BEAM SCRAPER UPSTREAM OF QF AT MINI-STRAIGHT
1000 GEV
SCRAPER: 6 CM(H), 20 CM(L)
$\phi = \pi$, $\theta_{BEAM} = -0.7$ MRAD
ϕ ANGULAR RANGE:
(●, ◇) 0.000 TO 0.100 RADIAN
(○, ▼) 3.042 TO 3.142 RADIANS
COIL RADIAL RANGE:
QUADRUPOLE DIPOLES
(●, ○) 3.81 TO 4.07 CM 3.81 TO 4.40 CM
(◇, ▼) 4.49 TO 5.00 CM 4.40 TO 5.00 CM
VACUUM CHAMBER RADIUS: 3.68 TO 3.81 CM
NO COLLIMATOR UPSTREAM OF DIPOLES
ENERGY DENSITY, GEV / (CM 3 . INTERACTING PROTON)
QF
DIPOLE
0
10
20
DISTANCE FROM UPSTREAM END OF QUADRUPOLE MAGNET (M)

Figure 28.

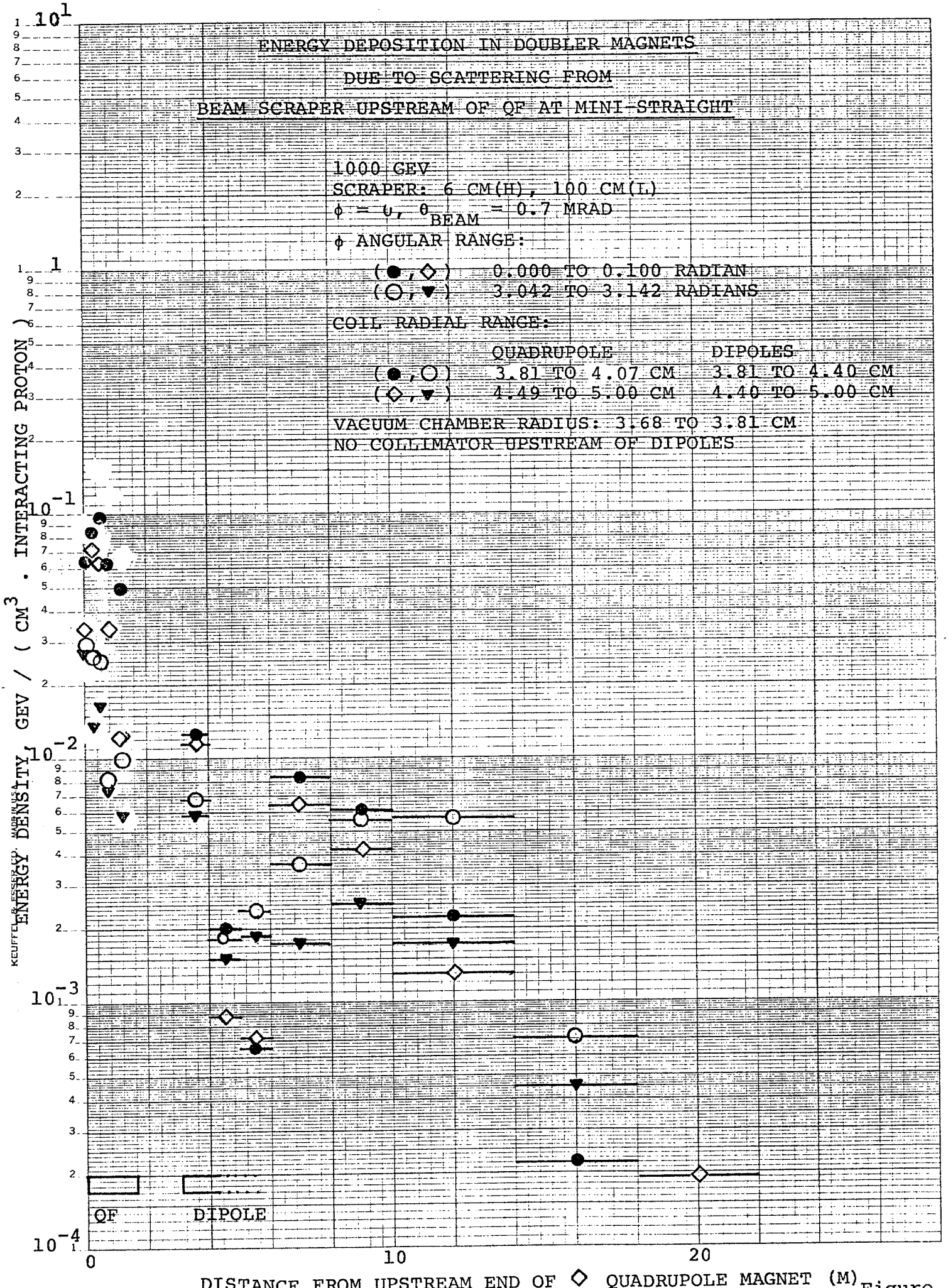
ENERGY DEPOSITION IN DOUBLER MAGNETS
DUE TO SCATTERING FROM
BEAM SCRAPER UPSTREAM OF QF AT MINI-STRAIGHT
1000 GEV
SCRAPER: 6 CM(H), 100 CM(L)
$\phi = \upsilon$, θ_{BEAM} = 0.7 MRAD
ϕ ANGULAR RANGE:
(●, ◇) 0.000 TO 0.100 RADIAN
(○, ▼) 3.042 TO 3.142 RADIANS
COIL RADIAL RANGE:
QUADRUPOLE DIPOLES
(●, ○) 3.81 TO 4.07 CM 3.81 TO 4.40 CM
(◇, ▼) 4.49 TO 5.00 CM 4.40 TO 5.00 CM
VACUUM CHAMBER RADIUS: 3.68 TO 3.81 CM
NO COLLIMATOR UPSTREAM OF DIPOLES
ENERGY DENSITY, GEV / (CM3 · INTERACTING PROTON)
KEUFFEL & ESSER CO. MADE IN U.S.A.
10^{1}
1
10^{-1}
10^{-2}
10^{-3}
10^{-4}
QF
DIPOLE
0
10
20
DISTANCE FROM UPSTREAM END OF ◇ QUADRUPOLE MAGNET (M)

Figure 29

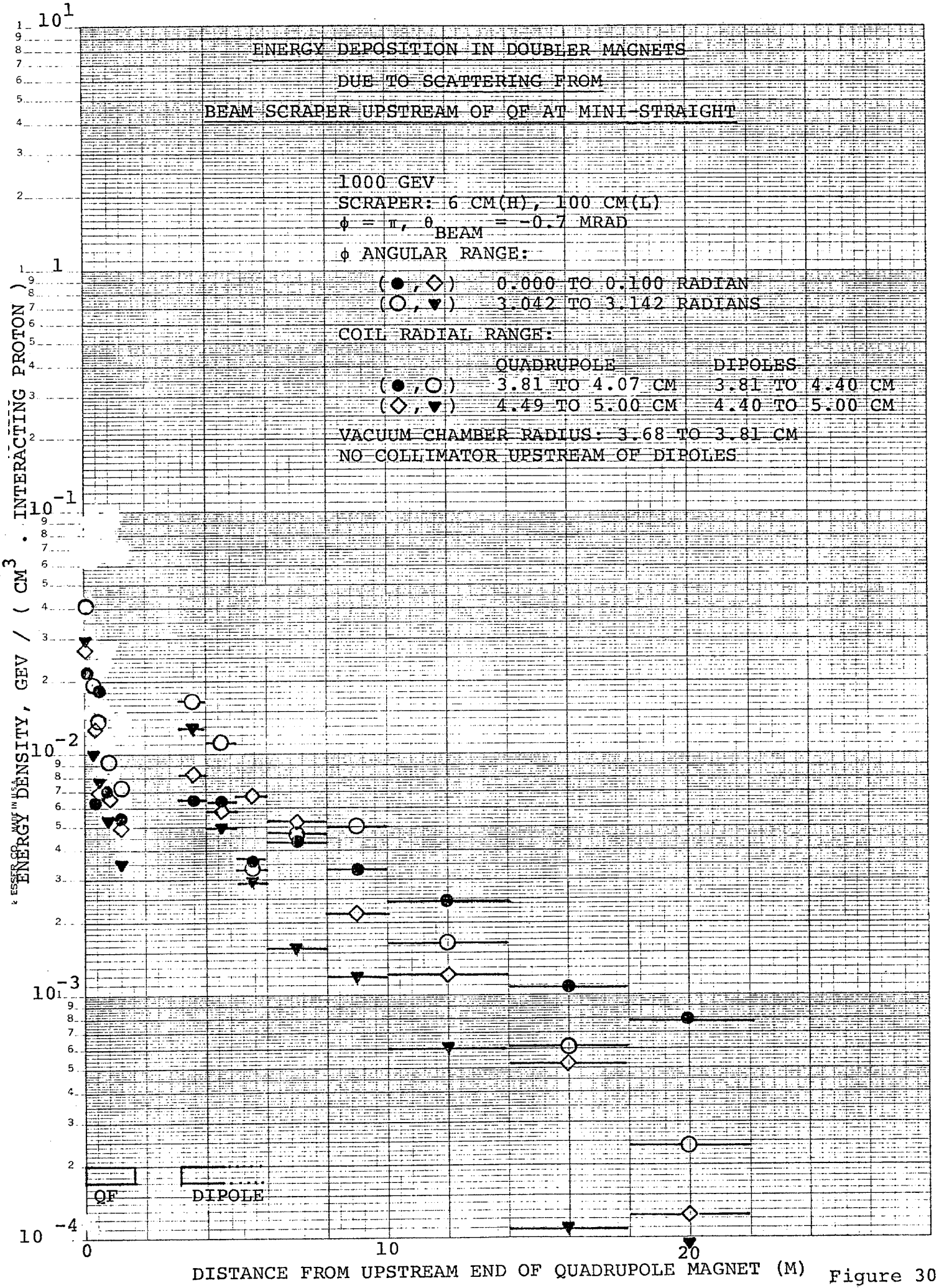
ENERGY DEPOSITION IN DOUBLER MAGNETS
DUE TO SCATTERING FROM
BEAM SCRAPER UPSTREAM OF QF AT MINI-STRAIGHT
1000 GEV
SCRAPER: 6 CM(H), 100 CM(L)
$\phi = \pi$, $\theta_{BEAM} = -0.7$ MRAD
ϕ ANGULAR RANGE:
(●, ◇) 0.000 TO 0.100 RADIAN
(○, ▼) 3.042 TO 3.142 RADIANS
COIL RADIAL RANGE:
QUADRUPOLE DIPOLES
(●, ○) 3.81 TO 4.07 CM 3.81 TO 4.40 CM
(◇, ▼) 4.49 TO 5.00 CM 4.40 TO 5.00 CM
VACUUM CHAMBER RADIUS: 3.68 TO 3.81 CM
NO COLLIMATOR UPSTREAM OF DIPOLES
ENERGY DENSITY, GEV / (CM^3 • INTERACTING PROTON)
10^1
1
10^{-1}
10^{-2}
10^{-3}
10^{-4}
QF
DIPOLE
0
10
20
DISTANCE FROM UPSTREAM END OF QUADRUPOLE MAGNET (M)

Figure 30.